Titre: Title:	Development of a Weldability Testing System to Quantify Hot Cracking Susceptibility of Inconel 718 Pre-Welded Sheets
Auteur: Author:	Hamzeh Fathollahzadeh
Date:	2015
Type:	Mémoire ou thèse / Dissertation or Thesis
Référence: Citation:	Fathollahzadeh, H. (2015). Development of a Weldability Testing System to Quantify Hot Cracking Susceptibility of Inconel 718 Pre-Welded Sheets [Mémoire de maîtrise, École Polytechnique de Montréal]. PolyPublie. https://publications.polymtl.ca/1729/

URL de PolyPublie: PolyPublie URL:	https://publications.polymtl.ca/1729/
Directeurs de recherche: Advisors:	Myriam Brochu
Programme: Program:	Génie mécanique

UNIVERSITÉ DE MONTRÉAL

DEVELOPMENT OF A WELDABILITY TESTING SYSTEM TO QUANTIFY HOT CRACKING SUSCEPTIBILITY OF INCONEL 718 PRE-WELDED SHEETS

HAMZEH FATHOLLAHZADEH

DÉPARTEMENT DE GÉNIE MÉCANIQUE

ÉCOLE POLYTECHNIQUE DE MONTRÉAL

MÉMOIRE PRÉSENTÉ EN VUE DE L'OBTENTION

DU DIPLÔME DE MAÎTRISE ÈS SCIENCES APPLIQUÉES
(GÉNIE MÉCANIQUE)

AVRIL 2015

UNIVERSITÉ DE MONTRÉAL

ÉCOLE POLYTECHNIQUE DE MONTRÉAL

Ce mémoire intitulé :

DEVELOPMENT OF A WELDABILITY TESTING SYSTEM TO QUANTIFY HOT CRACKING SUSCEPTIBILITY OF INCONEL 718 PRE-WELDED SHEETS

présenté par : FATHOLLAHZADEH Hamzeh

en vue de l'obtention du diplôme de : Maîtrise ès sciences appliquées

a été dûment accepté par le jury d'examen constitué de :

M. ACHICHE Sofiane, Ph. D., président

Mme BROCHU Myriam, Ph. D., membre et directrice de recherche

M. BROCHU Mathieu, Ph. D., membre

DEDICATION

"Everyone has a happy ending, if you are not happy then it is not the end."

To my wife: Nazanin Yadollahibastani, I couldn't have done this without you.

ACKNOWLEDGEMENTS

I would like to express my sincere gratitude to my supervisor, Professor Myriam Brochu for her guidance, technical and financial support, and helpful discussions during the course of this research.

I would also like to thank my loving wife, Nazanin Yadollahi, for her emotional support throughout all these years.

I extend many thanks to Pratt and Whitney for their support to provide required samples for my project.

And of course, I want to thank all the friends, professors, and classmates, who have been there through the good and the bad over these wonderful past two years.

RÉSUMÉ

Les défauts de fissuration à chaud sont fréquemment observés lors du soudage à l'arc sous gaz avec électrode de tungstène (GTAW), de feuilles d'Inconel 718. Dans le but de résoudre ce problème et d'améliorer la qualité des soudures, un projet de recherche a été mené par professeure Brochu de l'École Polytechnique de Montréal. Dans le cadre de ce dernier, des soudures ayant une variété de microstructures ont été produites en faisant varier les paramètres de soudage. Dans certaines de ces microstructures, un joint de grain central rectiligne a été observé : une caractéristique qui semblerait être à l'origine des fissures. Par la suite, des tentatives pour produire une soudure sans joint de grain central furent amorcées. Suite à ce projet, il a été jugé nécessaire de tester la susceptibilité à la fissuration à chaud des différents joints soudés. Ainsi, le but de ce projet est de développer un système et une méthode expérimentale permettant de déterminer l'effet de la microstructure de soudures existantes sur leur susceptibilité à la fissuration à chaud, et ce à un moindre coût. La procédure adoptée pour la conception et le développement du système est divisée en plusieurs étapes, soit l'analyse de la littérature et des méthodes d'essai de soudabilité existantes, la conception du système et le développement de la procédure expérimentale permettant d'évaluer les capacités du système.

En ce qui a trait à l'analyse de la littérature, les propriétés mécaniques de différents superalliages de nickel, particulièrement les alliages de type IN718, ont été comparées à d'autres matériaux. Les maints types de fissures pouvant se former lors du procédé de soudage de ces alliages ont ensuite été examinés. Les méthodes d'essai de soudabilité les plus courantes pour quantifier la sensibilité à la fissuration à chaud des matériaux y sont décrites. Il a été conclu de la revue de littérature que les méthodes d'essai impliquant l'application d'une contrainte externe sont plus efficaces que les autres puisqu'elles offrent un meilleur contrôle sur le déroulement du test.

Dans le chapitre suivant, les capacités et les limites des différentes méthodes décrites précédemment ont été analysées et comparées afin de vérifier leur capacité à répondre aux attentes et aux spécificités techniques du projet. Il a été conclu que la méthode d'essai de ductilité à chaud est celle qui répond au plus grand nombre de critères pour ce projet. Le chapitre 4 décrit le processus de conception de la méthode d'essai de ductilité à chaud qui comprend divers obstacles et défis qui ont dû être surmontés. Le chapitre concernant les procédures expérimentales et la mise sur pied du système fournit des détails sur certaines caractéristiques, et des spécifications quant

aux dispositifs et au matériel utilisés. Ensuite, l'assemblage des différents dispositifs est expliqué. Ce chapitre contient aussi des explications supplémentaires sur la procédure d'évaluation de la fonctionnalité et de l'efficacité du système.

Les résultats des tests ont montré que l'écart type maximum pour la mesure de la ductilité à chaud est de 6 et se produit à 1210ºC. D'autres essais ont été effectués sur deux microstructures soudées d'IN718 différentes pour valider la capacité du système à déterminer la susceptibilité à la fissure de solidification de différentes microstructures d'un même matériau. Les résultats ont confirmé qu'une microstructure soudée présentant un joint de grain central est plus susceptible de développer des fissures lors de la solidification de la soudure.

Finalement, des calculs plus détaillés ont été faits pour déterminer le budget requis pour créer et installer le système. Les résultats ont démontré qu'un budget d'environ 50,000$ est nécessaire pour développer ce système au département de génie mécanique de l'École Polytechnique de Montréal. De plus, le temps total requis pour déterminer la soudabilité d'un matériau par cette méthode est d'environ huit heures de travail, auquel il faut ajouter le temps nécessaire à la préparation de l'échantillon.

ABSTRACT

Hot cracking defects are frequently observed during the gas tungsten arc welding of Inconel 718 sheets. In order to solve this problem and improve the quality of the welds, a research project was carried out by prof. Brochu, École Polytechnique de Montréal. In their study, a series of welds with different microstructures were produced using various welding parameters. In some of these microstructures, longitudinal centerline grain boundary was observed: a characteristic that is seemingly a weak point for crack initiation. Subsequently, multiple attempts to produce a weld with no evidence of the centerline grain boundaries were initiated. Following up with the project by prof. Brochu, it was deemed necessary to test the hot cracking susceptibility of the different welds that were produced. Thus, this project's goal is to develop a system and an experimental method that are capable of determining the effect of the microstructure of the existing welds on their hot cracking susceptibility, and all of this at the lowest possible price. The procedure adopted to design and develop the system is divided in multiple steps, namely the literature review, the analysis of the existing weldability testing methods, the design of the system and the development of the experimental procedure allowing to evaluate the capabilities of the system.

In the literature review, the mechanical properties of several nickel base superalloys, particularly the IN718 alloys, were compared with other materials. The several types of welding cracks occurring during the welding processes of such alloys were then explained. The main part of this chapter describes the common weldability testing methods used to quantify susceptibility of the materials to hot cracking. It was concluded that the tests including the application of an external load are more efficient than the others since they provide a better control over the testing process.

In the next chapter, the capacities and the limitations of the different methods described above were analyzed and compared in order to verify their capability to satisfy the expectations and the technical specificities of this project. It was concluded that the hot ductility test is the method that meets the highest number of requirements of the project. Chapter 4 describes the designing process of the hot ductility testing system which includes various obstacles and challenges that had to be overcome during this endeavor.

The chapter concerning the experimental procedures and the system setup provides details about certain capabilities and on specifications concerning the devices and the equipment used. Then, the

assembly of the different devices is explained. This chapter also contains further explanations about the evaluation process of the functionality and the effectiveness of the system.

The test results showed that the highest standard deviation of hot ductility measurements is of 6 at 1210 ºC. Further tests were carried out on two different IN718 weld microstructures to validate the capability of the system to determine the solidification cracking susceptibility of different microstructures of the same material. The results confirmed that the weld microstructure with a longitudinal centerline grain boundary was more susceptible to weld solidification cracking.

Finally, more detailed calculations were made to determine the required budget to set up and install the system. The results showed that a budget of approximately 50,000$ is required to develop this system at the mechanical engineering department of the École Polytechnique de Montréal. Additionally, the total required time to determine the weldability of a material with this method is of about eight hours, to which the time required for sample preparation has to be added.

TABLE OF CONTENT

LIST OF TABLES

LIST OF FIGURES

LIST OF SYMBOLS AND ABBREVIATIONS

Symbols

σ_{th}	Threshold stress
μ_0	Magnetic permeability
μ_r	Relative permeability
S	Coil tube section
AB, A'B', A''B''	Pair reference points
aȧ, bḃ , cċ	Pair reference points
d_0, d_1 , d_2	Distance between the reference points
d_{ave1} , d_{ave2}	Rupture displacement average
D_i	Inside coil diameter
d_i	Inside coil tube diameter
D_o	Outside coil diameter
d_o	Outside coil tube diameter
e%	Elongation %
W	Weld width
W_h	Sample width in its head
W_{rc}	Sample width in its reduced section
x	Skin depth
δ	Elongation
δw	Resolution
ρ	Electrical resistivity
ω	Angular frequency

Abbreviations

ASTM	American Society For Testing And Materials
BRT	Brittle Temperature Range
CLGB	Center Line Grain Boundary
DAQ	Data Acquisition System
DRH	Direct Resistance Heating
DRL	Ductility Recovery Lines
DRT	Ductility Recovery Temperature
EBSD	Electron Backscatter Diffraction
EBW	Electron Beam Welding
GTAW	Gas Tungsten Arc Welding
HAZ	Heat Affected Zone
HCS	Hot Cracking Susceptibility
IH	Induction Heating
IN718	Inconel 718
IRH	Indirect Resistance Heating
MIG	Metal Inert Gas
NDT	Nil Ductility Temperature
NST	Nil Strength Temperature
PT	Peak Temperature
SAW	Submerged Arc Welding
SCS	Solidification Cracking Susceptibility
SCTR	Solidification Cracking Temperature Range
SD	Standard Deviation

INTRODUCTION

Aerospace engineers are always aiming to design jet turbine engines with higher capacities than their previous versions. Since these engines run at very high temperatures, they require special metal alloys capable of retaining their strength even at temperatures above 600°C. Nickel-based superalloys are one of the most important classes of engineering materials that can withstand these severe conditions. They are also widely applicable in rocket engines, nuclear power, chemical processing plants and other demanding environments [1].

In order to weld nickel and its alloys, most of the conventional welding processes can be used. However, gas tungsten arc welding (GTAW), metal inert gas (MIG) welding, submerged arc welding (SAW) and electron beam welding (EBW) are considered as the most common methods to weld these alloys [2].

The most important issue that limits the welding of these alloys is the presence of cracks either in the weld or near the fusion zone, in the heat affected zone (HAZ). Solidification cracking, liquation cracking and strain-age cracking are known as the most important cracking types to have been identified in these alloys [3]. Thus, studying the susceptibility of different materials to these types of welding cracks has always been an interest for many researchers. The varestraint test, modified cast pin tear test, Sigmajig test, hot ductility test and strain-to-fracture test are all well-known weldability testing methods.

Different weldability testing methods are designed to be applied for numerable testing conditions, sample geometries and materials. Therefore, many parameters such as the geometry of the material, the type of welding, the expected precision and the budget should be considered prior to selecting a method for weldability tests.

Problem statement

The industrial partner of this project has observed occurrence of the hot cracking defects during the GTAW of Inconel 718 sheet and forged component assembly. Thus, a research project was launched by Brochu et al. [4] to understand and improve the resistance of the joints to solidification cracking. Following a detailed characterization of cracked and uncracked specimens, it was proposed that center line grain boundary (CLGB) increases the weld susceptibility to solidification

cracking. In the second step of their research, it was attempted to promote a weld, free of center line grain boundary by modifying welding parameters. Finally, three different weld microstructures were produced, but no equipment was available to verify that the produced microstructures really improved the weld resistance to solidification cracking. Thus, the current research aims to develop a weldability testing system and method capable of quantifying hot cracking susceptibility of welds having different microstructures.

General objectives

The general objective of the current project is to develop a weldability testing system with less than 25,000$ which can be used to quantify hot cracking susceptibility (HCS) of pre-welded IN718 samples.

Specific objectives

The achievement of the following specific objectives will bring the project to completion:

- Identifying the best weldability testing method which meets technical requirements of the current project.
- Analyzing the system in terms of feasibility of developing the system at school.
- Evaluating of the system in terms of its testing precession and is capability to quantify solidification cracking susceptibility (SCS) of Inconel 718 samples.

Document organization

In the first chapter of this document, different types of welding cracks and the common methods of quantifying weldability of different materials are discussed. The second chapter outlines the limitations of each method to see which one is the best match for the requirements of this project. Then, in the third chapter, the possibility of applying various devices and equipment in the weldability testing system is explained and analyzed. The fourth chapter includes experimental and setup procedures through which the system is designed, developed and used to determine the weldability of different samples. Testing results and discussion are presented in the fifth chapter. This includes the results of hot ductility tests and the quantifying solidification cracking

susceptibility of two weld microstructures. Finally the conclusion, recommendations and future work are discussed.

CHAPTER 1 LITERATURE REVIEW

In this chapter, general properties of nickel base superalloys will be described and compared. It will be followed by the introduction of different types of cracks which usually occur during or after the welding of nickel alloys. Then, some important and widely used methods to determine the weldability of materials will be presented.

1.1 Nickle base superalloys

In the second and third decades of the 20th century, stainless steels were widely used for high temperature applications since a strong and corrosion resistant material was required. Advances in the aerospace industry were coincident with the improvement of engines capable of working at higher temperatures. The application of stainless steels was therefore limited since they could not exhibit desirable mechanical properties at temperatures above 540°C. In fact, their limitation in strength was a boost for the development of more heat resistant alloys. Superalloys are a good example of alloys developed specifically after World War II which were applied in aircrafts, industrial gas turbines and oil equipment. Superalloys are heat-resisting alloys which are grouped on the basis of their chemical composition. Today, nickel base superalloys represent about 50% of an aircraft engines' weight mostly due to their special metallurgy and mechanical properties [5].

In general, nickel based superalloys are divided into two major groups depending on their strengthening mechanisms:

- Solid solution strengthening,
- Precipitation strengthening.

Solid solution strengthened alloys exhibit moderated creep resistance (Figure 1-1) but good corrosion resistance up to 800° C. They are also widely used in power generation, chemical processing, petrochemical industries and composite tooling. *Precipitation strengthened alloys* exhibit outstanding corrosion resistance and high strength even at very high temperatures [3, 6]. Figure 1-1 indicates a 100 hours stress rupture behavior for three classes of superalloys [7]. The figure also includes the stress-rupture behavior of carbide-phase-strengthened cobalt alloys which is not of any interest for this research.

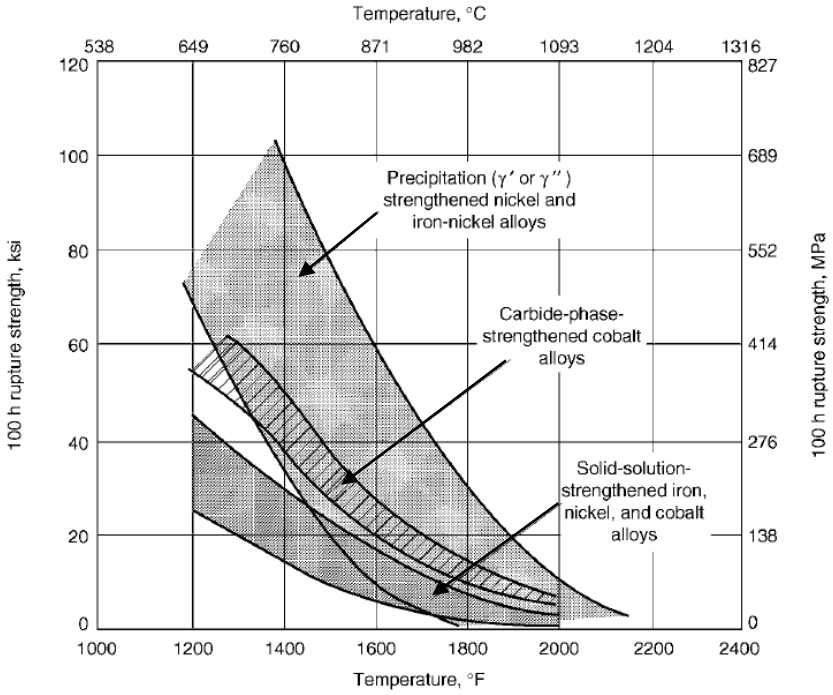

Figure 1-1 : Stress-rupture behavior of three classes of superalloys [7]

1.2 Welding of superalloys

Welding is often used to manufacture components from superalloys. Cost effectiveness and successful manufacturing is therefore highly influenced by the alloy weldability. One of the common welding methods in the aerospace industry is GTAW. This welding process is very interesting for this project since it was used to produce different weld microstructures by using different welding parameters as will be explained bellow.

In the welding process by GTAW, a power supply is used to create an electric arc between a non-consumable tungsten electrode and a work piece (Figure 1-2). The energy created by the power supply melts the metals and produces a weld. An inert shielding gas (Argon and Helium) is used to protect the weld area (fusion zone and heat affected zone) from atmospheric contamination. Depending on the application, a filler metal can be used (Figure 1-3). When no filler material is required, the method is called autogenous welding.

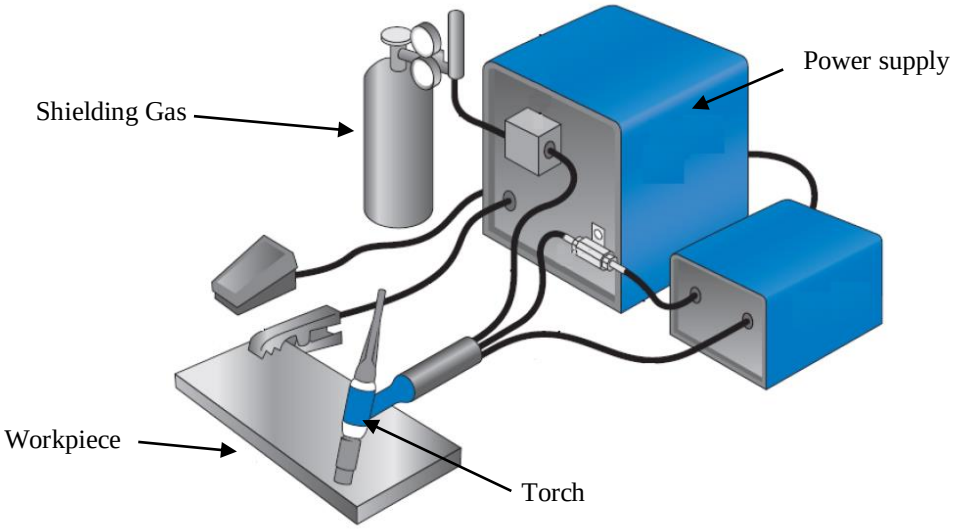

Figure 1-2 : GTAW system [8]

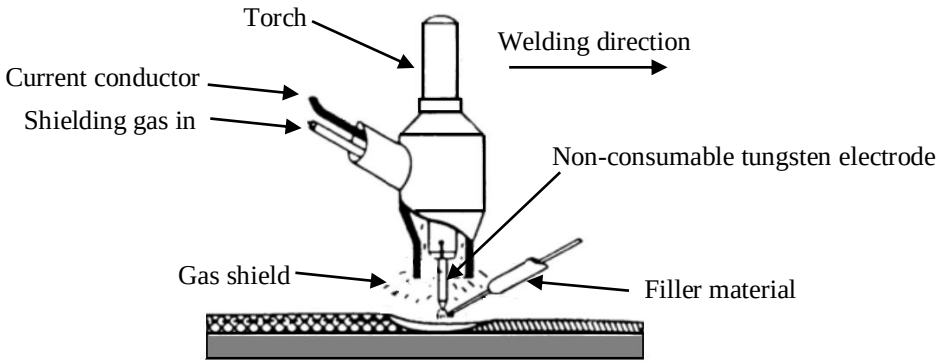

Figure 1-3 : GTAW torch in operation [9]

There are three main variables which can be used in welding process by the GTAW. The first variable is the arc voltage, which is the voltage between the tungsten electrode tip and the work piece. The arc current and length, the type of shielding gas and the shape of the tungsten electrode tip can influence the arc voltage. The second variable is the welding current which can be used to get a desired welding penetration. Depending on the material and thickness of the metal base and the geometry of the electrode, various welding currents may be applied. The speed at which a torch (Figure 1-3) is moved along the joint is the last variable, called the welding speed. The shape of the weld pool and width are important characteristics of a weld which are affected by the welding speed.

1.3 Welding defects and cracks

Most defects which occur during welding of nickel-base superalloys are cracks. Although the quality of a weld can be influenced by a wide variety of defects (undercut, inadequate fusion and porosity), cracks are one of the worst types of defect since a failure can be caused by the growth of a small crack. One of the factors that contribute to the formation of a crack is the material's insufficient ductility in combination with tensile stresses. Thus, the temperature at which a crack initiates can be used to categorize different types of cracks. Based on these temperatures, cracks can be categorized into two main groups: hot and cold [10].

1.3.1 Cold cracking

These cracks usually occur in solid state near or at room temperature, in a state where no liquid film is in the weld. Excessive strain in the weld after cooling can also promote the formation of cold cracks. This is typically observed in welds of a very thick cross section with presence of a high temperature gradient during welding.

Figure 1-4 (a) and (b) show the typical locations of a cold crack in a weld and its heat affected zone (HAZ). Transverse cracks are typical of excessive strains in the thick cross section samples. Toe[1] and underbead[2] cracks usually occur in the weld heat affected zone. They are likely to be caused by a combination of excessive stress and a brittle HAZ [11].

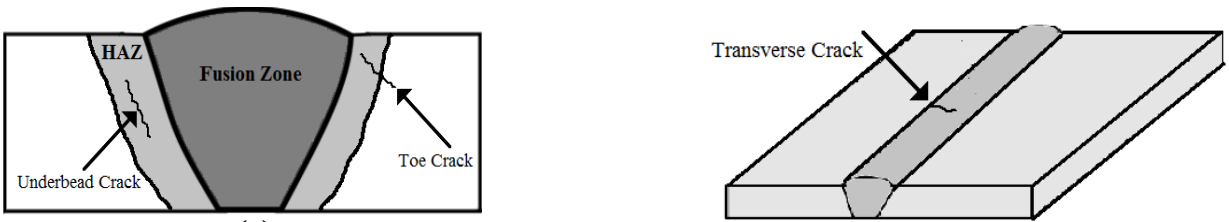

(a) (b)

Figure 1-4 : Cold cracks locations in (a) cross section and (b) surface of a weld (inspired from [10])

[1] Where the base metal ties in to the weld metal along the weldment face.

[2] In a weld HAZ under and adjacent to its fusion zone.

1.3.2 Hot cracking

Hot cracks form in the weld fusion zone and heat affected zone due to the formation of the liquid in the system at high temperatures [3]. In fact, during solidification where shrinkage stresses are induced in the weld by high cooling rate, hot cracks can initiate at different weld locations. Transverse, longitudinal and crater[3] cracks are some examples of the hot cracking defects [11] shown in Figure 1-5 (a) and (b).

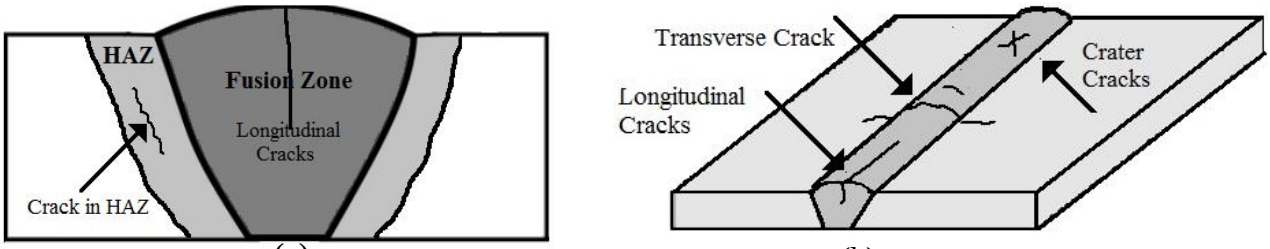

Figure 1-5 : Hot cracks in cross section (a) and surface (b) of a weld (inspired from [10])

Hot cracking generally occurs in two regions of a weld, both susceptible to the formation of liquid films:

- The fusion zone (Solidification cracking susceptible region),
- The partially melted region in heat affected zone (Liquation cracking susceptible region).

1.3.2.1 Solidification cracking

Many of the weld cracks formed during weld fusion are associated with boundaries and interfaces of alloys. Figure 1-6 (a) shows solidification of grain boundaries in the fusion zone which can affect susceptibility of an alloy to solidification cracking. During solidification, shrinkage strains are induced by phase transformation from liquid to solid and thermal contraction within the weld. At the same time, low melting point liquid films form along solidification grain boundaries. If the mushy zone[4] ductility is inferior to these deformations, cracks initiate at the final stage of

[3] The end of a welding pass where the weld pool is unfilled.

[4] Solid-liquid region which forms during welding and trails behind the liquid weld pool.

solidification [4]. Figure 1-6 (b) shows the fusion zone and beginning of solidification. The figure also shows a solidification crack caused by the presence of shrinkage strains.

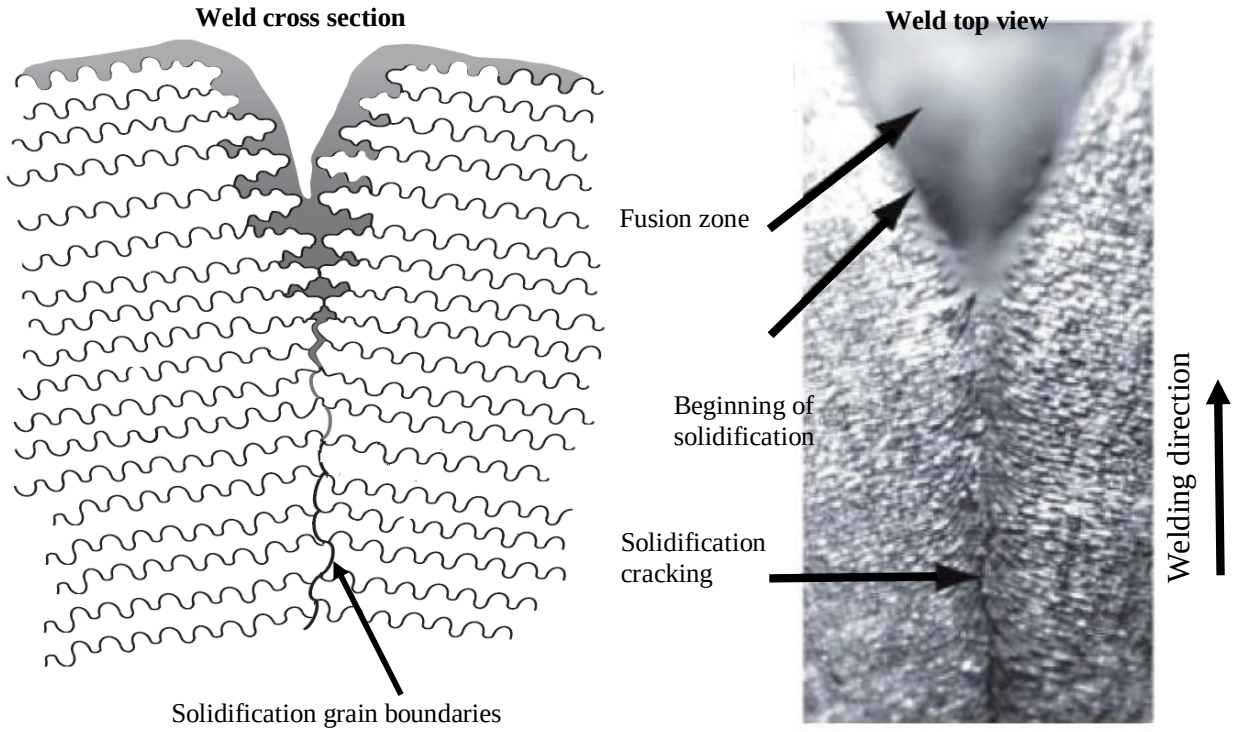

Figure 1-6 : (a) Solidification grain boundaries in a weld metal [12]. (b) Formation of solidification cracking during welding process [13].

Generally, solidification temperature range is one of the major metallurgical factors affecting the susceptibility of the weld to solidification cracking. The temperature range directly affects the size of the mushy zone. At the beginning of the mushy zone, the temperature is equal to the liquidus temperature. On the other side, the end of the mushy zone intersects with the lower temperature of an alloy where the weld is completely solidified. Higher temperature ranges can induce larger volumes of the mushy zone, thus enhancing the susceptibility to solidification cracking [3].

1.3.2.2 HAZ cracking

In order to evaluate the base metal susceptibility to HAZ cracking, the resistance of a metal to the formation of liquation cracking should be studied. Liquation cracking happens when the hot ductility of a metal is lower than the high-temperature induced strains. The presence of liquid films

within the base metal during solidification is necessary to the formation of liquation cracks. The higher solidification temperature ranges can increase the presence of liquid films in base metal [3].

1.4 Weldability testing methods

The weldability of a material exhibits its resistance to crack formation, the more an alloy is weldable, the less cracks it is likely to form during welding.

In order to measure and compare the weldability of different materials, many testing methods have been developed. Those methods are usually used to quantify the HCS can be categorized into two groups of self-restrained and externally loaded tests.

In self-restrained tests, no load is externally applied to the samples and cracks are formed only by shrinkage strains during solidification. Cast pin tear test is an example of such a test [14].

In order to carry out an externally loaded test, samples which are usually machined into particular shapes are mechanically tested by applying external loads. With this method, it might be necessary to test specimens in a particular thermal-cycle. The transvarestraint, Sigmajig, U-type hot cracking and hot ductility tests are all examples of externally loaded tests that will be discussed in this section.

1.4.1 Modified cast pin tear test

In this test, a gas tungsten arc welding torch is used to melt small charges of material. A water cooled copper mold is then used as a recipient for the molten materials. In order to determine cracking susceptibility, different restraints can be generated by controlling the length of the molds (Figure 1-7). The longer pins can potentially create higher solidification restraint and lead to the formation of circumferential cracks on the outside of the pins (Figure 1-8). All the obtained information regarding the pin length and its associated circumferential cracking percent can be presented in a plot (Figure 1-9) [14].

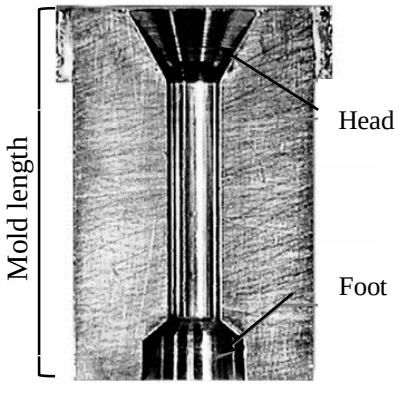

Figure 1-7 : A mold of cast pin tear test [15]

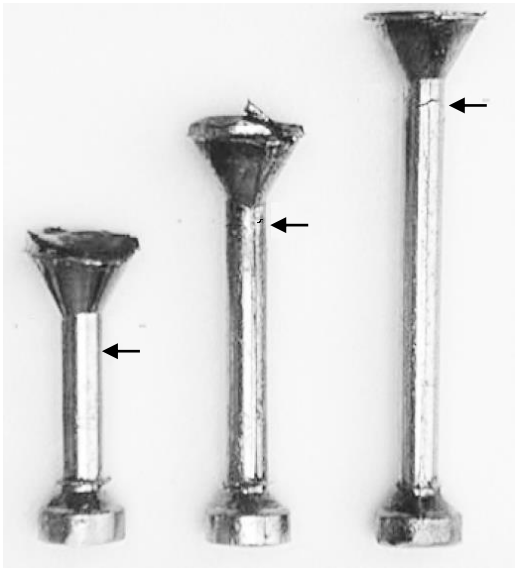

Figure 1-8 : Locations of cracking in different cast pins shown by arrows [14]

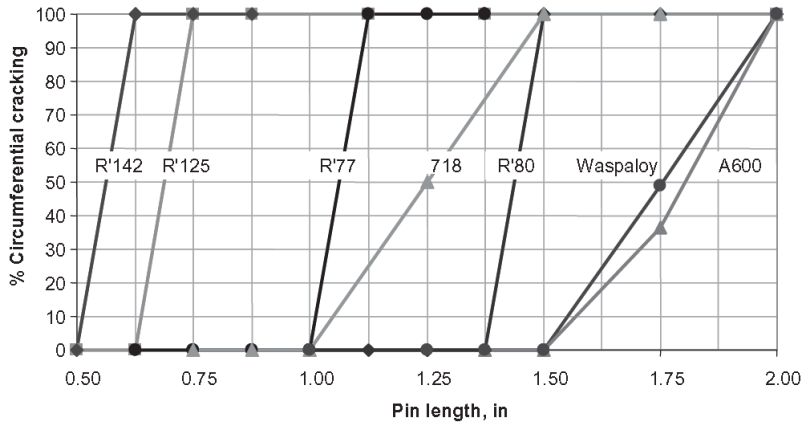

Figure 1-9 : Results of modified cast pin test for different alloys [15]

According to Figure 1-9, the most susceptible materials to solidification cracking are those where cracking occurs all around the diameter of the pin (100% circumferential cracking) at the shortest pin length [14, 15]. This test only verifies weld solidification cracking of materials with different chemistry. In fact, it is a quantitative test since no material properties are measured.

The cast pin tear test can only be used to determine solidification cracking susceptibility of a cast material. In fact, it is not a method that can be used to quantify the weldability of various welds. Basically, the welding process includes microstructural evolution within the welded area which may result in inhomogeneous mechanical properties in the weld, base metal and heat affected zone. This can promote residual shrinkage strain within these regions which affects the weldability of the material. Still, the cast pin tear test is considered as one of the simplest and less expensive methods. It is mainly used in studies that have aimed to obtain a general understanding of the susceptibility of a material to solidification cracking.

1.4.2 Varestraint test

Varestraint test was first developed by Savage and Lundin in 1960 to quantify HCS of materials [16]. This method is generally performed based on augmented strains rather than on metallurgical variables at the root cause of hot cracking. Figure 1-10 (a) shows a Varestraint testing machine with a welding ram, mandrel die and a testing sample. The movable welding ram produces a weld on the sample which is bent to get the shape of a mandrel. The increased strains generated by bending loads cause cracks to occur on the outer surface of the under welding sample (Figure 1-10 (c)). The most commonly used welding process for these tests is GTAW whose welds are usually autogenous[14].

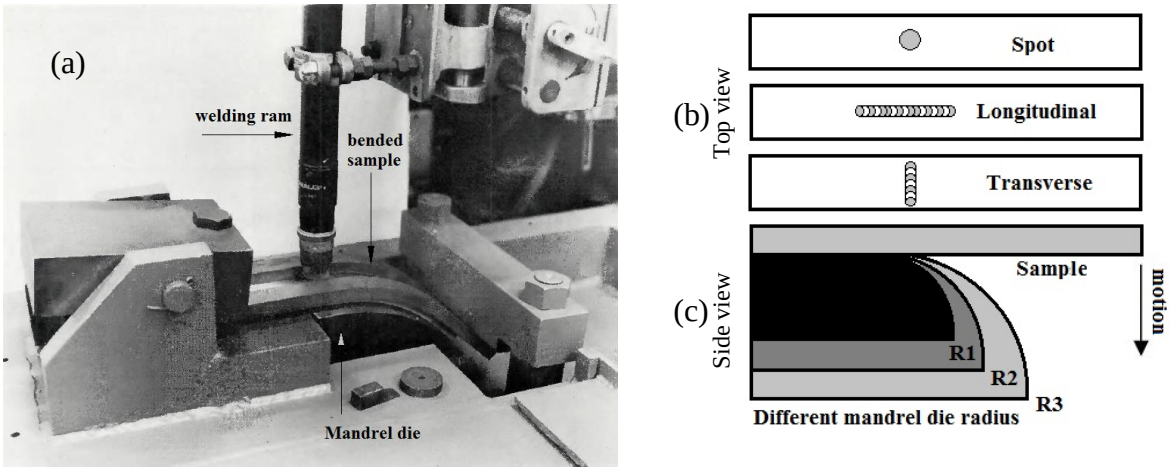

Figure 1-10 : (a) A varestraint testing machine [17]. (b) The direction of welds relative to the applied augmented bending strain. (c) A schematic of the Varestraint testing machine showing its different mandrel die radius (inspired from [18]).

As it was partially explained, the Varestraint test rapidly applies bending strains that promote cracking on the outer surface of a sample. The relative direction of the applied strain and welding determines the susceptible region in which cracks occur. Based on this, the Varestraint test can be divided into three types of longitudinal, transverse and spot tests as shown in Figure 1-10 (b).

In the longitudinal type, bending strains are applied along the length of the weld. This would promote cracking in both the fusion (solidification cracking) and heat affected zones (liquation cracking). In order to separately determine the susceptibility of these types of cracks, two other methods known as transverse and spot Varestraint tests can be used[14].

In the transverse test, bending strain is imposed perpendicularly to the weld and circumscribes most of the cracks in the fusion zone (Figure 1-11 (a)). Extension loads are perpendicular to the partially melted zone (the most susceptible region) causing longitudinal cracks in the fusion zone. In order to promote cracking in the heat affected zone, a spot Varestraint test was developed (Figure 1-11 (b)). This method involves bending a sample in which a small melted spot weld was created [3]. As Figure 1-11 (b) demonstrates, the extension load on the outer surface affects the partially melted zone surrounding the spot in the HAZ.

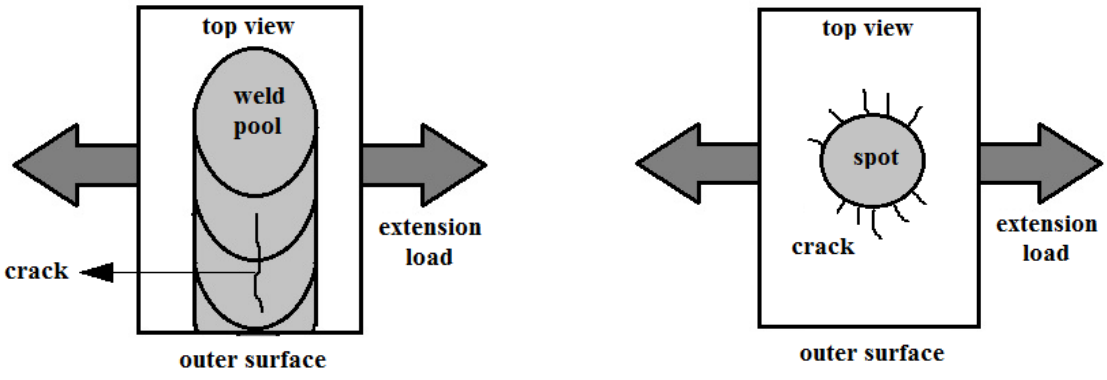

(a) (b)

Figure 1-11 : The stretched surface of two samples showing crack propagation in (a) transverse and (b) spot test.

1.4.2.1 Testing Procedure

The general procedure of Varestraint test can be described as follows:

- Fix the specimen in a testing machine (Figure 1-10 (a)). It should be mentioned that the samples of 3mm thick or less are not recommended to be tested on with this method to avoid buckling during bending [3, 16]. Other samples dimensions, such as length and width, can be selected based on the capacity of the testing machine.
- Produce weld on the specimen while welding pool temperature is measured by a thermocouple. It should be noted that the temperature is measured only if the purpose of a test is to determine brittle temperature range which is explained in this section.
- Apply the bending strains to the specimen. Tension strains intensity on the specimen outer surface is controlled by the mandrel dies of different radiuses which is shown in Figure 1-10 (b).
- Observe cracks by 25-40x magnification.
- In order to get significant and accurate results, three to six tests are usually carried out for each strain level.

1.4.2.2 Evaluation of weldability

Different parameters have been used by researchers as indicators to evaluate the HCS by Varestraint test. All these indicators come from observations of cracks formed either in a weld or in the heat affected zone. For instance, the number of cracks, the maximum crack length, the total crack length and the average crack length are some of the measurements used to evaluate and compare materials HCS [6, 17-22]. For example, if comparing different alloys, it would help to determine which material contains the shortest crack length, and ultimately find the most weldable material.

In addition, the temperature range in which solidification cracking initiates and propagates may be measured. This is called the solidification cracking temperature range (SCTR) which can be obtained by measuring the maximum crack length and temperature course in a weld (Figure 1-12). In this regard, the temperature of the weld pool can be measured by a thermocouple. This can be used to plot time-temperature graph. Then, the longest crack in all tests is divided by the welding travel speed to get the time interval in which the crack occurred. Now, by merging the information of the weld pool time-temperature graph with the material's solid temperature and cracking time interval, the temperature range in which a crack may develop in the mushy zone can be determined [19]. The wider this temperature range, the lowest weldability for a material is anticipated.

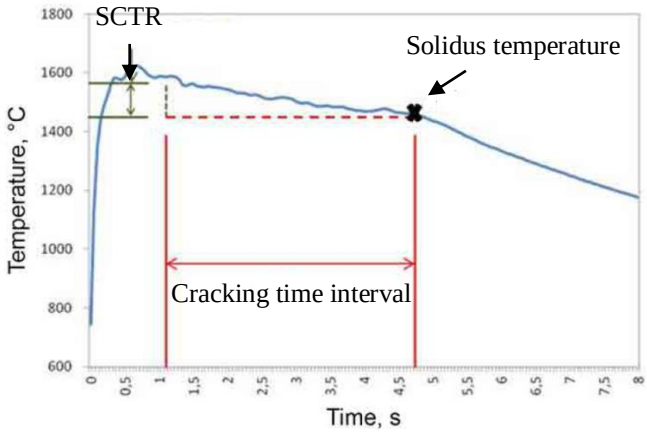

Figure 1-12 : The methodology through which temperature of liquid metal pool is monitored and SCTR is measured [19].

The general limitations of weldability testing with the Varestraint method can be described as follows:

- This method is limited to specimens thicker than 3mm. Otherwise, buckling[5] may occur during bending when the samples cannot perfectly get the shape of the mandrel.
- Actual strain on the outer surface of the specimen is always different from the ideal value since the sample cannot perfectly take the shape of the mandrel block during bending. It causes different radius values between sample and die. Therefore, to get better estimation of actual applied strain, a correction factor may be required.
- Varestraint test is an operator sensitive method since its final testing results is highly dependent on the operator's decision on the number and length of cracks.

1.4.3 Sigmajig

Figure 1-13 shows schematic representation of a weldability testing system that was developed by Goodwin [23] in order to evaluate solidification cracking susceptibility of thin sheet metals (less than 0.25mm) [24]. Instead of taking measurements of cracks and/or determining the solidification temperature range, mechanical load frame of this test is used to measure the stress at which a crack initiates in a weld (Figure 1-14). This stress, called threshold stress σ_{th}, can be used to compare cracking susceptibility of different materials.

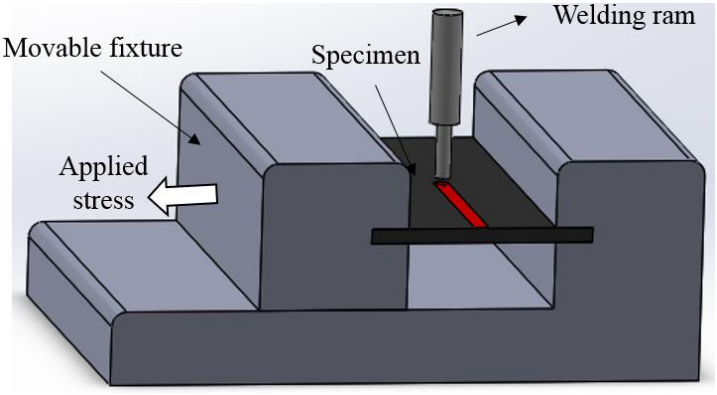

Figure 1-13 : Schematic of a Sigmajig testing fixture (inspired from [23]).

[5] Excessive bending in a compression portion of a member when the applied load remains unchanged.

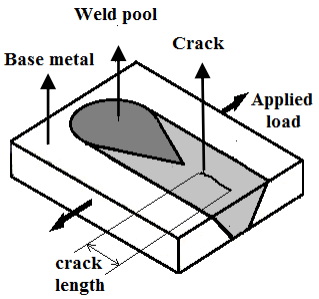

Figure 1-14 : Fusion zone crack induced by an external load in the Sigmajig test

1.4.3.1 Testing procedure

- Small square shaped samples (50mm×50mm) are clamped between hardened steel grips (Figure 1-13).
- Before loading, it may be verified that the gas tungsten arc facilities will produce a full penetration and teardrop-shaped weld in the samples [23]. It is important since it leads the cracks to concentrate on the weld centerline, therefore causing solidification cracking.
- Predetermined loads are applied to the sample and then measured through a pair of strain gauges.
- If no crack is observed, the load level is increased by 50lb per each 1-mm thickness of the sample. This process should be continued until cracking is visually observed in the sample [24, 25].
- The minimum stress at which cracking occurs in the specimen is reported as the threshold stress.
- When cracking occurred in the sample, additional tests must be conducted with 10lbs above and below the respective load in order to verify the threshold stress [24, 25].

1.4.3.2 Evaluation of weldability

As stated above, threshold stress in the Sigmajig test is used to evaluate the solidification cracking susceptibility of a material. In that regard, results are usually plotted based on cracking percentage versus applied stress. Figure 1-15 shows the diagrams of two different materials where cracking percentage increases with increasing stress until the point at which complete separation occurs. There are two important indications in this plot which show that the material 2 is more weldable

than the material 1. Firstly, cracking occurs at lower stress levels in material 1. Secondly, it exhibits a more gradual transition from the first occurred crack to the complete separation point (100% cracking).

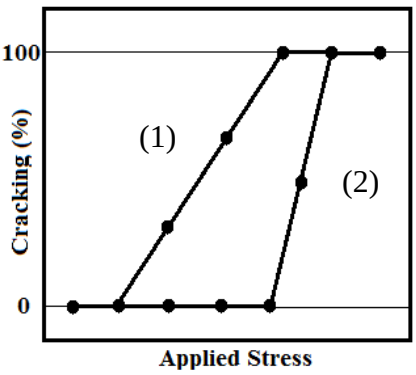

Figure 1-15 : A typical Sigmajig testing diagram indicating that the material 2 is more weldable than the material 1 [14]

Generally, this method is designed to quantify SCS. In addition, since a testing specimen is subjected to a preload during the welding process, the Sigmajig method is limited to bead on welds therefore butt welds cannot be tested.

1.4.4 U-type hot cracking test

The U-type hot cracking tester was developed in Hiroshima University in order to quantify the SCS without using a mechanical load frame [26]. Since the Varestraint is not precise enough to determine local strain at trailing edge of the weld pool, this method can determine local strain in the vicinity of cracking lips during GTAW welding [27]. In fact, this setup can generate solidification cracking at the center line of a weld by applying an extension load transverse to welding direction of the sample. It should be noted that in a manner similar to those of the other weldability tests (Transvarestraint and Sigmajig), the load is applied to a specimen while welding. Then, through measuring the local critical strain at the crack initiation area, susceptibility to solidification cracking is determined. In order to determine the critical strain, two grains are taken as reference points using a high magnification microscope installed on the high speed camera for observation. The critical strain can be determined using the distance between reference points before and after the fracture.

This testing setup usually contains the following devices to evaluate the weldability of a metal:

- U-type hot cracking tester,
- Laser autogenous welding equipment,
- High speed camera.

In Figure 1-16, a schematic of the U-type tester configuration is shown where a specimen can be fixed between the ends of two beams using chucking plates. If the beams are bent towards each other, the extension strain can be applied to the sample after it is fixed completely between them. This strain will promote solidification cracking in the sample during welding. In addition, a laser welding machine is generally used to produce autogenous welds [2].

Meanwhile, a high speed camera is used to record the process in which a crack forms in the sample. It is then possible to retrieve the recorded film to determine the critical strain in the cracking area [28]. Figure 1-17 shows the full setup of a U-type hot cracking test using a high speed camera and a laser welding machine. A metal halide lamp is also used to provide adequate light for better filming quality.

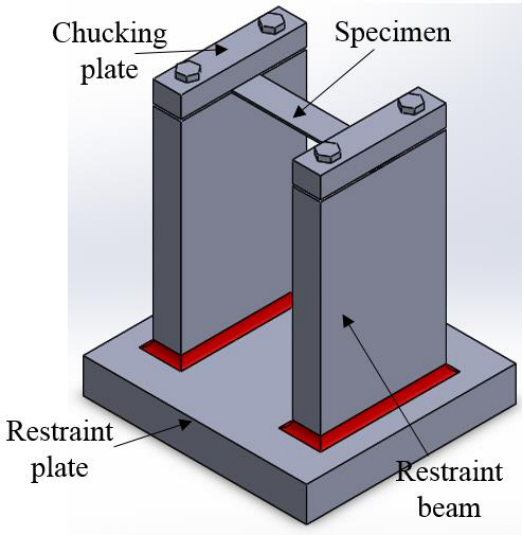

Figure 1-16 : General schematic of the U-type tester configuration (inspired from [2])

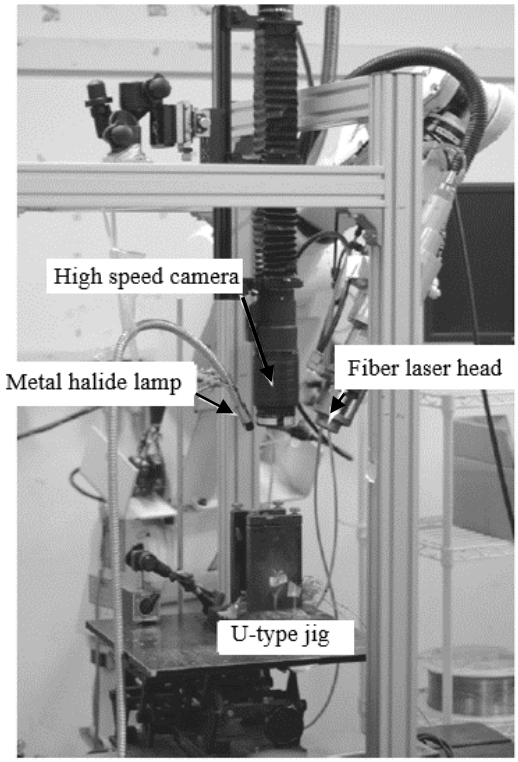

Figure 1-17 : U- type hot cracking test setup [28]

1.4.4.1 Testing procedure

- Fixing the sample between the free end of one of the beams and the respective chucking plate.
- Pushing two ends of the beam towards each other and at the same time fixing the other end of specimen to the free end of the second beam.
- Welding the middle of the sample. In the case of evaluating solidification cracking, welding travel direction must be normal to the direction of extension strain (similar to Sigmajig and Transvarestraint methods in solidification cracking tests.)
- Using the high speed camera to record process of crack formation which normally occurs behind the welding pool in the centerline of the weld.
- Retrieving the film to measure displacement of the reference point (grains) to determine critical strain.

- In the case of measuring brittle temperature range, a platinum thermocouple is used to measure temperature interval during which the critical crack occurs. The process is similar to the methods used to quantify SCTR in Varestraint test.

1.4.4.2 Evaluation of weldability

Figure 1-18 shows displacement of reference points when cracking occurs in the weld due to the applied strain. In the figure, d_1 and d_2 are the distance between the reference points, respectively before welding and after the formation of the crack. The difference between d_1 and d_2 is used to measure the critical strain at which a crack is initiated in the weld. Based on the results of this test, the materials which exhibit the lower level of critical strains are more susceptible to weld solidification cracking [2].

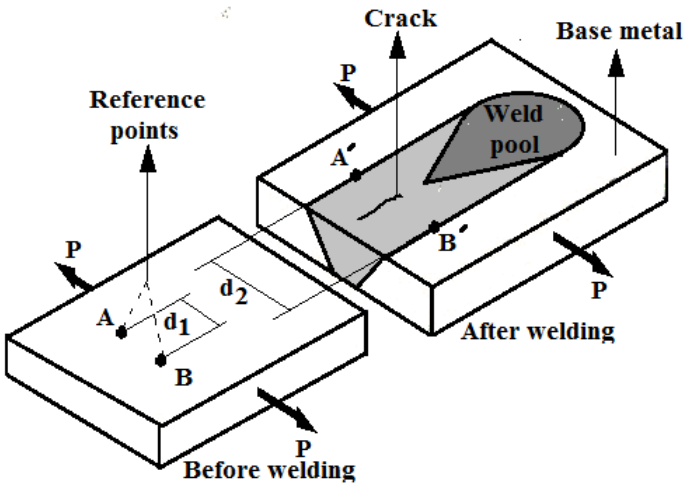

Figure 1-18 : Measurement of reference points displacement in a U-type hot cracking test

With this method, the welding travel speed should be taken into consideration in the final analysis. In fact, different cracks can occur at various welding speeds within the weld and the HAZ. This phenomenon might make it necessary to conduct further observations in order to recognize a particular type of crack. Besides, it is impossible to apply constant strain on the specimen during the U-type jig since the applied strains decrease by increasing the bending radius of the beams. Moreover, because of the preload applied to a sample this method is limited to bead on welds.

1.4.5 Hot ductility test by Gleeble

Elevated temperature properties of a material such as hot strength or hot ductility[6] can be used to evaluate its weldability. The typical machine used to test hot ductility properties of a material is Gleeble which is shown in Figure 1-19. This machine can mechanically test a sample at different temperatures over a thermal cycle [29].

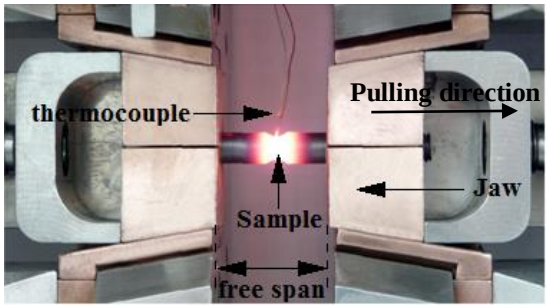

Figure 1-19 : Hot ductility test by a Gleeble machine[29]

1.4.5.1 Thermal system

In a Gleeble test, samples are heated by a high electrical current that passes through them. As Figure 1-19 indicates, a sample is placed between two jaws which are connected to a high current circuit. The figure also shows a thermocouple which is welded to the center of the sample. It is used to monitor and control the temperature. Besides, to avoid the system from overheating, a chiller pumps water through the jaws.

Depending on the jaws' material and the length of free span, temperature distribution over the sample will change. Figure 1-20 (a) shows parabolic temperature distribution over the length of a sample in which the highest temperature is at the center. For example, once compared to stainless steel jaws (hot jaw), it is found that copper jaws (cold jaw) result in a steeper curve because of their higher thermal conductivity [30].

[6] Elongation of a sample subjected to a specific temperature and strain rate.

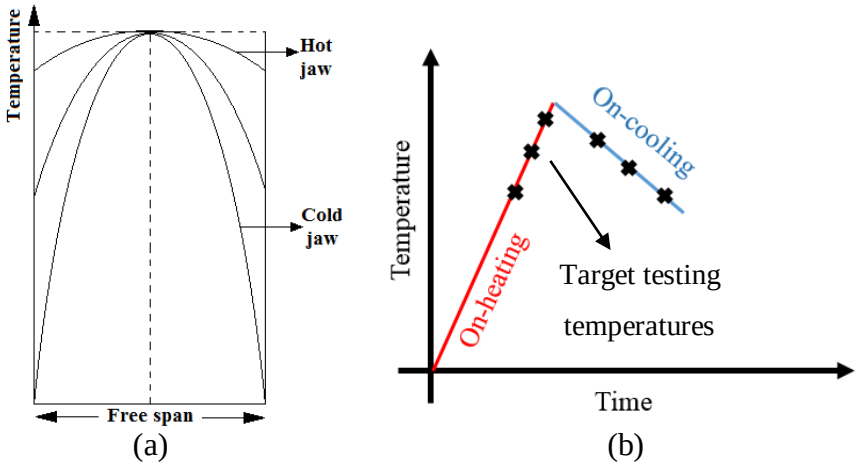

Figure 1-20 : (a) Heat distribution over a sample in the free span with the cold and hot jaws [30]. (b) The thermal schedule over which the samples are fractured at various target testing temperatures

1.4.5.2 Mechanical System

The mechanical system of Gleeble is capable of applying tension to a sample along its center axis through jaws. One of the jaws is fixed and the other one is attached to a hydraulic ram whose movement can be monitored by stroke, force or strain. During the simulation of a thermal cycle, a mechanical system can apply controlled displacement or load to a sample at different temperatures (Figure 1-20 (b)) [31].

1.4.5.3 Thermal cycle simulation

The general purpose of this test is to characterize the ductility of a material at elevated temperatures. This can be used to quantify the hot cracking susceptibility of a material, usually presented as ductility versus temperature plots. Figure 1-21 indicates a typical hot ductility plot including on-heating and on-cooling curves. Over the on-heating tests, the material shows increasing ductility which dramatically drops to zero after the peak point. At this temperature, known as Nil Ductility Temperature (NDT), the material exhibits no ductility. Another point in this diagram is Nil Strength Temperature (NST), the temperature at which the material exhibits no strength.

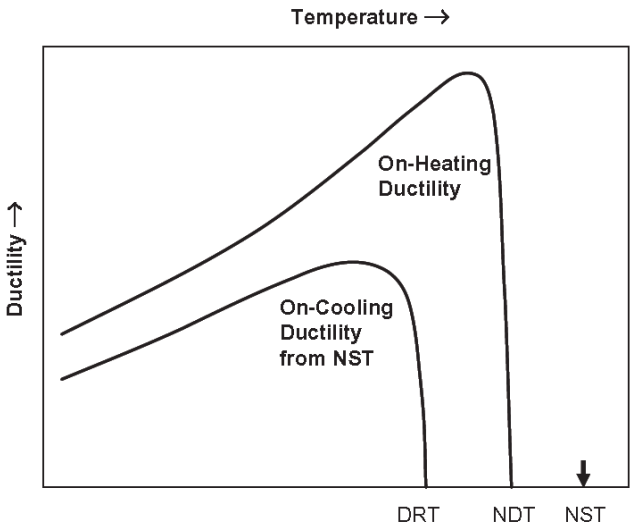

Figure 1-21 : Typical on-cooling and on-heating ductility curves [14]

Further tests on on-cooling lead to the determination of the Ductility Recovery Temperature (DRT) point. In order to determine this temperature, a specimen is heated to NST and then cooled. During the cooling process, specimens are pulled to fracture at various temperatures. After different tests, a certain temperature is determined as the point at which the material starts to retrieve its strength. That point on the plot can be reported as DRT.

1.4.5.4 Testing procedure [14]

- Testing sample should be machined into a standard geometry which can be fixed between the jaws.
- Weld fusion zone is located in the center of the sample where the peak temperatures usually occurs.
- On-heating tests are usually carried out by a heating rate of about 111ºC/sec and pulling the sample at different desired testing temperatures by a stroke rate of 50mm/sec.
- NST can be determined by heating at a rate of 111ºC/sec while a constant tension stress is applied to fracture a sample.
- For the on-cooling tests, samples are heated at the rate of around 111ºC/sec up to a peak temperature and then cooled at a rate of almost 50ºC/sec. During cooling process samples are fractured at 25℃ interval with the stroke rate of 50mm/sec.

- Dimensions of fracture area are then measured to determine the ductility of samples based on the reduction area.

1.4.5.5 Evaluation of weldability

Hot ductility curves provide valuable information on a material's weldability. The temperatures of NDT, NST and DRT can define crack susceptible regions. For example, the difference between two temperatures of NST and DRT indicates the temperature range over which grain boundary liquid films are presented in the material. The wider the temperature range, the higher the susceptibility to hot cracking in the HAZ can be predicted for a material [3, 6, 32]. However, the more exact way to predict this is by comparing hot ductility curves. The on-cooling curves are more important since hot cracks usually occur during cooling process. One of the methods is to quantify the rate at which a material retain its ductility. The faster a ductility recovers, the less susceptible it is to form a hot crack.

In general, the first limitation of this test is the application of high heating and cooling rate, which may alter the properties of the materials and especially those which encounter microstructural evolution at high heating or cooling rates. In addition, Gleeble is an expensive multipurpose thermal-mechanical simulator that is used not only for weldability tests but also in a wide variety of applications ranging from physical simulation such as hot rolling of steel and aluminum to research into high temperature performance of metal alloys for jet engines. Therefore, if weldability evaluation is the only purpose of a research, the investment is not reasonable; this will be detailed in the next chapter.

1.5 Conclusion

As explained in the literature review section, externally loaded testing methods are better to control the testing procedure and to provide more precise measurements of weldability. In addition, they can be more precise in measurements aimed to study the effects of different welding parameters on the weldability. For example, in the Varestraint, Sigmajig and U-type hot cracking tests, weldability of different welding parameters can be directly quantified, whereas in the hot ductility tests by Gleeble different welding parameters are indirectly simulated on a specimen. Therefore, externally loaded testing methods seem more likely to fulfill the expectations required to achieve the main objective of the current study. However, more analysis should be made in terms of capability of the systems to meet requirements of the project.

CHAPTER 2 ANALYZING THE EXISTING WELDABILITY TESTING METHODS

In this chapter, more detailed analysis will be made on the weldability testing methods in terms of their capability to meet the requirements of the current project. The results of analysis will then be used to find the best method to achieve the project goal which is "developing a cost effective weldability testing system to quantify HCS of pre-welded IN718 samples".

To achieve the goal, the weldability testing system must exhibit the following capabilities and specifications:

1st: Quantifying the hot cracking susceptibility of thin pre-welded samples.

2nd: Measuring the weldability of welds produced by changing the welding parameters.

3rd: Necessitating low monetary investment (less than 25000$) and reasonable testing time.

2.1 Quantifying hot cracking susceptibility of a thin pre-welded sample

If the purpose of this study is to understand how different weld microstructures can influence cracking susceptibly, a testing method needs to be sensitive enough to determine small variations of HCS.

The cast pin tear test is a method to evaluate the weldability of a material's chemistry rather than of a welded microstructure.

The Varestraint, Sigmajig and U-type hot cracking methods consist of breaking a sample while welding and are not designed to test a pre-welded sample.

Gleeble can be used to test pre-welded samples since it is capable of simulating actual welding conditions in the welded area.

2.2 Measuring the weldability of welds produced by different welding parameters

With the Varestraint and Sigmajig tests, the effects of different welding parameters on a material's weldability can be directly tested. The control allowed on the direction of the applied stress or strain can determine and ensure the occurrence of a crack whether in the fusion or the heat affected zone.

Different welding parameters can be indirectly tested by Gleeble. The machine can be programed to simulate and test different welds produced by various welding parameters, such as heat input and welding travel speed.

2.3 Testing time and cost

In order to get an estimation of the required budget to conduct the mentioned weldability testing methods, the total testing cost is assessed based on the required equipment and the total testing time.

2.3.1 Required equipment and specimen preparation

In this part, direct and indirect cost of different externally loaded test will be analyzed. The overall cost of each method was estimated based on the required testing equipment and the sample preparation. Table 2-2 contains the information on the sample preparation and the major equipment required for different tests.

In order to fix samples between two jaws of the Gleeble machine, samples needs to be machined into specific geometries (threaded end rod samples or pin holes made at two ends of samples) [33], whereas the other tests use simple square or rectangular shape samples. Consequently, samples with more complex geometries are more expensive and may increase the machining cost.

Concerning the required equipment to carry out a weldability test, the U-type testing method uses more equipment and devices than Varestraint and Sigmajig tests, which makes the testing procedure more complex and expensive. The Gleeble machine, being a multipurpose thermal-mechanical physical simulator, is considered as the most expensive method for weldability tests. Table 2-1 includes an approximate range of testing costs for each method.

Table 2-1 : Required samples and equipment in externally loaded methods

Type of test		**Varestraint**	**Sigmajig**	**U-type**	**Hot ductility with Gleeble**
Crack type		Solidification and liquation	Solidification	Solidification and liquation	Solidification and liquation
Sample geometry	**Shape**	Rectangular	Square	Rectangular	Rod or Rectangular with complex geometry
	Thickness	$> 3mm^a$	$> 0.25mm^a$	$> 0.25mm^a$	NS^b
	Width & length	Flexible^c	$50 \times 50mm$	NS^b	Rod length is usually 100mm but the others are Flexible^c
Equipment	**Welding or welding simulator**	Autogenous welding machine	Autogenous welding machine	Autogenous laser welding machine	• Electrical resistance heater • Water cooled quenching system
	Mechanical testing	Bending machine^d	Testing jig^f	U-type jig	Servo-mechanical testing system
	Measurement process	• Thermometer ^{f} • Microscope	Microscope	• High speed camera • Thermometer ^{f}	• Any device to measure reduced cross section or elongation
Approximate testing cost		\$30K-\$40K	\$30K-\$40K	\$40K-\$50K	\$500K-\$1M

a: upper range is limited by capability of testing machine
b: not specified and generally depends on machine's limitations
c: restricted by machine's maximum capabilities
d: with different mandrels of various radius
e: capable of applying different loads
f: not necessary only if the brittle temperature range is of interest

2.3.2 Required testing time

The required time to complete the weldability tests is analyzed based on the required time (1) to setup a system and make that ready for a test and (2) analyze its final results. Table 2-2 compares the required time at each step of different weldability tests.

Gleeble has the simplest procedure to conduct a test since all of the required equipment is gathered in a single machine. All of the testing parameters such as heating rate, cooling rate and stroke rate can be programmed and automatically applied in a testing procedure. Further analysis is only needed to measure a reduced cross section or the elongation of a sample after fracture.

In the Varestraint and Sigmajig tests, most of the required time for initial setup is spent on pre-adjustments of the welding machine to ensure that appropriate welding speed and depth are achieved. The U-type test has more measurement equipment, like a high recording speed camera, which increases the required setup time.

Because of the application of a high speed camera in the U-type test, the final analysis of the fractured sample is relatively fast and simple. In all other tests, further time consuming processes are required for the observation and inspection of fractured samples to make measurement of cracks or cross section.

Table 2-2 : Required time for each step at different weldability methods, valued from 1 (lowest) to 4 (highest)

Type of test	**Varestraint**	**Sigmajig**	**U-type**	**Hot ductility with Gleeble**
Sample preparation	3	2	1	4
Setup	3	2	4	1
Total testing procedure	3	4	2	1
Final analysis	4	3	1	2

2.4 Conclusion

The design and development process of the weldability testing system of the current study is followed through a systematic engineering design approach [34]. Table 2-3 shows the first stage of this procedure.

After identifying the project's requirements and clarifying the overall task, background research was carried out on different weldability testing methods. This step has been achieved by analyzing said methods to find possible solutions for existing problems. At this stage a check list, as shown in Table 2-3, was prepared to compare the capability of each method to achieve the objectives of the present project.

Table 2-3 : The procedure followed to find the potential research problems

Objectives	Background research	Results		
		Specifications		
		1st	2nd	3rd
1-Quantifying HCS of pre-welded samples 2-Quantifying HCS of different welding parameters 3-Having total testing equipment of less than 25,000$	Cast pin tear test	×	×	√
	Varestraint test	×	√	×
	Sigmajig test	×	√	×
	U-type hot cracking test	×	√	×
	Hot ductility with Gleeble	√	√	×

Therefore, it can be concluded that the hot ductility test with Gleeble is the method with the highest number of potential solutions for the existing problems. Despite the machine being too expensive, it is the best candidate for the weldability testing of a thin pre-welded sample among all of the other analyzed methods.

It has now been evaluated that it is worthy to design and customize a weldability testing system to quantify the weldability of different weld microstructures at the lowest possible price.

CHAPTER 3 DESIGN METHODOLOGY AND CHALLENGES

In chapter 2, the analysis of the existing solutions showed that the hot ductility test is the best option to determine the weldability of pre-welded samples. In the design and development process of the system, two important factors need to be considered: price and precision. The system should be developed at the lowest possible price but should remain precise enough to determine the HCS of different microstructures. After the goals were set, a systematic approach [34] was used to achieve them. Firstly, the required specifications of the hot ductility testing system were identified. Secondly, the specific problems and millstones hindering the achievement of the project's objectives were clarified. This was followed by the identification and analysis of the possible solutions for the existing problems. The third and final step consisted of selecting the best equipment possible based on the advantages and limitations of each solution.

As explained in Chapter 1, a hot ductility testing system should possess the following capacities to quantify the HCS of a weld.

Capacity of:

1) producing a welding thermal cycle
2) mechanically testing samples
3) precisely measuring ductility

In addition, the total cost of the system should be less than 25000$. Thus, the total cost of equipment for the system should stay within the defined budget by the client.

3.1 Producing a welding thermal cycle

One of the required specifications of a hot ductility testing system is its capability to simulate a welding thermal cycle. Thus, it must be equipped of a heating and/or cooling system in order to produce the high heating and cooling rate.

3.1.1 Heater

During on-heating or on-cooling tests, the sample is fractured at a target temperature after having experienced a predetermined thermal cycle. Since the application of these thermal cycles is to simulate the actual welding conditions, the approximate heating rate of the welding process should

be quantified. The testing heating rate, applied by other researchers, is about 110°C per second [3, 6, 24, 35-37]. This value can be used in testing the weldability of pre-welded samples.

Besides, the heater should be capable of heating a workpiece to its melting point. Since most of engineering metals melt at about 1600°C, especially those widely used in gas turbine engines, it is essential for the heater to reach this temperature.

The capability of a heater to localize the heat within the weld and in the heat affected zone is another required specification if the weldability of different microstructures is of interest. This region's width may vary approximately between 5-15 mm and is associated with different welding widths and applied heat input.

In addition, the heater should not disturb the performance of other equipment, especially instrumentation devices.

Electric heaters are controllable, clean and efficient. Different types of this kind of heater are explained in this section.

3.1.1.1 Indirect resistance heating (IRH)

Depending on the application and testing requirements, different equipment can be used to heat an object in a laboratory environment. The most common way consists of using an electric laboratory oven. In these types of ovens, a piece of equipment converts electric current to heat. Since by this type of heaters the heating rates of about 110°C/s cannot be achieved, other type of heaters should be considered. Amongst high heating rate heaters, there are two important systems: the direct resistance heating and the induction heating. In these heating systems, the majority of the total energy converts to heat inside the material.

3.1.1.2 Direct Resistance Heating (DRH)

In the direct resistance heating system, an electric current flows through an electric conductive material and directly heats the sample based on the Joule Law[7]. Typically, metal is clamped to electrodes in the walls of a furnace and charged with electric current. The electric resistance within

[7] An electric current through a resistor converts electrical energy into heat energy.

the load generates heat in the work piece. The temperature can be controlled by adjusting the electrical current. The Gleeble machine uses this system which can heat specimens at rates of up to 10,000ºC/sec [33].

3.1.1.3 Induction Heating (IH)

Basically, in an induction heating system, a solid state power supply provides an alternating current in a coil, and the load is placed inside the coil. This causes magnetic fields to enter the load and induce circulating eddy currents within the part. These currents flow against the electrical resistivity of the metal, generating precise and localized heat without any direct contact between the part and the coil. Heating rates can be controlled by varying the frequency and power of the current in the coil[38].

3.1.1.4 Analysing the heaters

Table 3-1 includes capabilities and specifications of the mentioned heaters and the related analysis is explained as follow:

Table 3-1 : Comparison of the different heating system

Heaters	**Max heating range (1600°C)**	**Heating rate (110°C/s)**	**Heating zone (5-15mm)**	**Availability**	**Uniform heating profile**	**Safety**
IRH	No	No	No	Yes	Yes	High
DRH	Yes	Yes	Yes	No	Yes	Low
IH	Yes	Yes	Yes	No	No	Moderate

Heating rate: The heating rate of the IRH is lower than the one of the other heaters. In an oven for example, a material's surface is heated first and then as a result of the existing thermal gradients the rest of the material heat up gradually. In the direct resistance and induction heating systems,

electric current flows through an electrically conductive material and heats it directly. This increases their capacity to reach higher heating ranges and heating rates.

Heating zone: In the DRH, the heating zone can be determined by adjusting the distance between two grips. Since grips can be made from materials of high thermal conductivity, the heat can be concentrated between the grips. A localized heating profile can also be achieved by IH methods but through a different method. In IH, the width of the heating zone depends on the one of the magnetic field, which is applied to the mass in the center of the coil. Thus, selecting coils of smaller width would promote heating in the smaller portion of the sample (Figure 3-1 (a) and (b)).

(a) (b)

Figure 3-1 : Different width of coils with a load inside (a and b)

Safety: Concerning the safety issues, the DRH method can potentially cause more hazard compared to the IH method. High current/voltage electricity passes into the sample and is in contact with grips and other metallic parts of the testing machine. This may cause electrical shock, while an induction heater provides a noncontact heating of the work piece.

Uniform heating profile: With the IH method, eddy currents are greater at the surface and decrease towards the center. This phenomenon is called skin depth and can be calculated by Equation (3-1).

$$x = \sqrt{\frac{2\rho}{\omega \mu_0 \mu_r}} \qquad (3\text{-}1)$$

Where x (meter) is the skin depth, ρ is the electrical resistivity (Ω-meter), ω (Hz) is the angular frequency of a coil current, μ_0 (newtons per ampere squared) is the magnetic permeability and μ_r is relative permeability of the testing material. Therefore, when testing thick samples, skin depth should be calculated to make sure that a uniform heating profile can be generated throughout their cross section.

Moreover, since in the DRH method, the electrical current is applied to the sample through grips, a misalignment of the sample in its longitudinal direction would increase the applied bending strains to the sample. The other problem occurs at a shortened distance between grips, a distance which is adjusted to generate smaller heating zones. This can interfere and limit the application of different instrumentation devices such as thermocouple and extensometers since they need a certain amount of space to be installed in the system. In addition, in order to create the desired heating profile in a weld and a heat affected zone, several parameters such as grips material, optimal grips distance and sample material and geometry should be taken into account. Lastly, electrical current can affect the functionality of thermocouples which are usually welded to the sample.

3.1.2 Cooler

A typical welding process consists of a very rapid heating (several hundreds of degrees per second) to peak temperature, followed by a relatively fast cooling (a few tens or hundreds of degrees per second) to ambient temperature. Due to these high cooling rates, the microstructure of the weld and heat affected zone may change.

Microstructural changes in the weld and the heat-affected zone (HAZ) are greatly dependent on various welding parameters such as the weld heat input (a function of arc energy, travel speed and thermal efficiency of the process), the plate thickness/geometry and its initial temperature. Therefore, in order to determine the weldability in different welding conditions, hot ductility parameters (heating and cooling rate) should be chosen as close to reality as possible.

On the other hand, if the purpose of a test is to determine HCS of different weld microstructures, hot ductility parameters (heating and cooling rate imposed during a test) should not change the microstructure of pre-welded samples. In this case, the applied thermal cycle to a pre-welded sample should be in a range in which the weld's microstructure would not be changed. The approximate cooling rate used by other researchers is around 50°C/s [3, 6, 36, 39, 40].

In the Gleeble machine, electrical currents flow through a sample and heat the whole part. The distance between the high thermal conductivity grips is controlling the cooling rate and generating a desired heating profile over the sample. If the heating zone can be localized to the welded region, cooling a sample in the air would simulate the most similar heating profile to the real welding condition. Thus, it would not be necessary to cool a sample using a cooling system.

3.1.3 Thermometer

A successful hot ductility test is highly influenced by a thermometer used to measure the temperature during tests. The thermometer for a hot ductility test should have at least two important technical features: measuring temperatures at high temperatures and with high frequency sampling.

Since the melting point of most of the existing metal does not exceed 1600°C, a thermometer should precisely measure temperatures up to this level. It should also possess maximum accuracy and precision of the elevated temperatures at which the hot ductility tests are performed.

The other limitation in choosing a thermometer is its sampling rate. Mechanically testing samples at different temperatures when they undergo high heating rates can make the testing process very short. In this short time and at the very small temperature interval, the testing system must be capable of determining adequate and precise data points which will be used to extract ductility-temperature curves. For example, for a heating rate of 100°C/s, a thermometer should be able to read temperature changes at least every 10ms. This is to avoid measuring identical values at same temperatures and having the thermometer precise enough to detect every degree of temperature changes.

There are two common devices used to measure and monitor the temperature of specimens during on-heating and on-cooling process: the thermocouple and the infrared pyrometer.

3.1.3.1 Thermocouples

Depending on the temperature range and the heating rate, different thermocouple types can be chosen. The most common thermocouples in Gleeble are type K, S, R and B. Up to 1250 C, tests can be run using type K thermocouples. According to Omega's recommendation, types R and S can be used continuously in an oxidizing or inert atmosphere up to 1400ºC. Type B is rated for continuous use up to 1704ºC in an oxidizing or inert gas atmosphere. When operating near these maximum temperatures, the heavier gage wire sizes are recommended.

3.1.3.2 Infrared pyrometer

Infrared pyrometers determine the temperature of an object by measuring the amount of infrared energy emitted by the object [41]. They provide the possibility of measuring the object's temperature by distance. Consequently, they are useful for measuring temperatures under

circumstances where thermocouples cannot be used or do not produce accurate data. Some typical circumstances include the followings:

1- The object is surrounded by an electromagnetic field, for example when using an induction heater.

2- A fast response is required.

3- The temperatures are above the point where thermocouples may be damaged or melt.

4- Contact with a thermocouple may damage the object.

5- Contact with the surface of the object induces a noticeable temperature gradient which leads to a significant measurement error.

3.1.3.3 Analyzing the thermometers

General specifications on different thermometers are presented in Table 3-2. The technical numbers are mean values only used to get a general understanding of their compatibility to be applied to the hot ductility testing system.

Table 3-2 : Comparison of the different thermometers

Specifications	**Wire Size (mm)**	**Max Temperature (ºC)**	**Response speed**	**Resolution (ºC)**	**Availability at school**	**Safety**
K-type thermocouples	0.13	1250	1s	0.1	Yes	High
B-type thermocouples	0.51	1700	20s	0.1	No	High
Infrared pyrometer	-	1600	1ms	0.1	No	High

Max temperature: As it was explained, maximum measurable temperature by a thermocouple depends on its wire size. The thicker a wire is, the higher a working temperature can be reached. On the other hand, thicker wires have a slower response time.

Response speed: Although a type B thermocouple, can withstand temperatures of up to 1700ºC, its response time is still far away from the required technical specification of the hot ductility testing system.

Moreover, both direct resistance and induction heaters can influence the measurements of a thermocouple. Since thermocouples are usually welded to the sample, high electrical current or high density magnetic fields can disturb the induced electrical current in a thermocouple tip. In addition, the presence of any conductive material in the magnetic field of an induction coil can affect the heating performance and efficiency of an induction heater.

Despite the capacity of the infrared thermometers to satisfy the technical requirements of the system, having a precise and accurate measurement necessitates the emissivity of the device to be carefully adjusted.

3.2 Mechanically testing samples

In the thermal cycle produced by the hot ductility testing system, specimens are pulled to fracture at a constant strain rate. In the hot ductility tests conducted by other researchers, standard specimens were fractured at a pulling speed of 50mm per second [3, 6, 36, 40] (For various free span lengths the strain rate may vary from 1 to 2/s). Depending on a sample's geometry, different methods such as a using a tensile testing machine or a testing jig can be taken to apply the stroke rate to the sample. Tensile testing machines, which are usually available at laboratories of engineering schools, are capable of testing samples at different strain rates. Moreover, in the Sigmajig and U-type hot cracking tests, a special jig is used to hold and apply various strain rates to specimen. In this kind of jig, the exact level of the subjected strain to a sample is determined by the application of strain gauges. Therefore, depending on the testing condition, the budget and the expected precision of the previously mentioned mechanical systems can be used.

3.3 Precisely measuring ductility

If the goal of research is to quantify the HCS of different welds, the hot duality testing system must be capable of measuring the ductility of the pre-welded samples. This can be feasible if the system shows the following capabilities: localizing the heat in the welded region and quantifying the ductility of the material in that region.

In addition, the system should be capable to automatically control the testing procedure. This is important since mechanically testing samples at different distinctive temperatures over the thermal cycle makes the testing period very short and complex.

3.3.1 Extensometer

A successful hot ductility test ends by an accurate and precise measurement of ductility. Welding a sample can change mechanical properties locally and, more particularly, change the ductility pattern of a metal within the welded region. Various welding parameters may produce welds with different ductility. In order to determine the weldability of a weld, the testing system must be sensitive enough to measure the ductility of a weld.

In general, the ductility of a material can be reported by the percentage of elongation. In order to precisely measure the ductility of a weld, the gauge length of an extensometer should be equal to the weld width. If δw (mm) is the measurement resolution[8] and w_0 (mm) is the gauge length of the extensometer, the measurement error can be calculated by Equation (3-2).

$$error\ (\%) = \frac{\delta w}{w_0} \times 100 \tag{3-2}$$

In this case, for a given resolution, if the gauge length decreases, the error percentage increases. In order to achieve an expected precision, the extensometer must exhibit higher resolution.

There are three methods which can be used to determine the rupture ductility of a material such as stroke transducer, contact and video extensometers.

3.3.1.1 Stroke transducer

Tensile testing machines are used LVDTs to measure the motion of the piston. If the displacement of the piston is used to determine the length changes of a specimen, the compliance of the machine is also included in the final results. Higher loads create larger machine deformations and increase measurement error. This type of error can be even worst at higher temperatures since the testing

[8] The finest change in length that can be measured by an extensometer.

specimen gets softer. In this case much more deformation is included in the measurement, to a point where it is only desirable to determine the deformation of the weld.

3.3.1.2 Contact Extensometer

Extensometers are widely applied to precisely measure the elongation of a region in a specimen. The clips on these devices remain on the specimen to measure very high rupture displacement (up to 1000 mm). Resolution of these devices is typically of about 0.3 µm.

High temperature extensometers are also available for measurements at elevated temperatures. The problem of measurements at such high temperatures occurs when the clips of the contact extensometer are forced on the specimen. This deforms the sample, which gets softer because of the elevated temperatures, and causes errors in the final results. In order to overcome this problem, other extensometers providing a non-contact measurement of the elongation can be used.

3.3.1.3 Video extensometer

Video extensometers can measure the elongation on any preferred region of a sample with no physical contact. The device is equipped with a camera used to continuously capture images of the specimen during the test. The specimen can be marked using special tools or markers. These marks, which are distinguishable from specimen color, will be tracked in the captured video or images to measure the elongation. With the proper installation of a camera towards the subject and depending on the type of camera that is used, a resolution of at least 1µm can be achieved.

3.3.1.4 Analysing the extensometers

Table 3-3 compares some specifications of the aforementioned extensometers. Based on the presented information in said table, the extensometers were analyzed as follows.

Table 3-3 : Comparison of the different methods to measure the elongation

Extensometer	**Resolution**	**Mean elongation**	**Sampling rate**	**Selective measurement region**	**Availability**	**Output signal**	**Safety**
Stroke transducer	0.1μm	100mm	1KHz	No	Yes	Yes	High
contact extensometer	0.3μm	10mm	1KHz	Yes	Yes	Yes	High
video extensometer	1μm	300mm	1KHz	Yes	No	Yes	High

Resolution: If the goal of a test is to determine the elongation of a weld microstructure, a smaller gauge length is required. Then, for an expected testing precision, an extensometer of a higher resolution should be selected.

Mean elongation: Selecting the mean elongation range of an extensometer depends on the maximum elongation of the weld at rupture. The range should be high enough to assure that the displacement of the reference points will be captured until fracture. This is important especially when a video extensometer is used.

Sampling rate: A high sampling rate is important for testing procedures that are very fast. For example, to indicate an exact rupture elongation by a video extensometer, the sampling rate should be high enough to determine the rupture moment of the specimen which happens faster than milliseconds.

As it was explained, stroke transducers cannot provide a reliable measurement of the elongation, especially at high temperatures. In addition, the clips of contact extensometers which is forced to a sample may deform a thin sample at elevated temperatures. Thus, among the mentioned candidates, only video extensometers meet the expected technical requirements of the current research. Despite all of the mentioned advantages, it is not always easy to measure high temperature elongations with a high speed recording camera. For example, some parameters should be perfectly adjusted while testing with a video extensometer, such as ambient light and orientation of the static

camera towards the target. An inappropriate selection of the mentioned parameters can influence final testing results. In addition, these kinds of devices are very expensive and are not available at school.

In order to overcome this problem, it is possible to take the principles of testing by video extensometer and apply them to tests done with another method. Continuing with this idea, as shown in Figure 3-2, two reference points within a known distance from each other can be marked on specimens. After the rupture, the two fractured parts can be put back together and, by measuring the distance between A'' and B'' (d_2), the final elongation can be obtained [42]. When testing with such a method, many errors can alter the measurement. For example, it is not always possible to perfectly put back together the fractured surfaces, which can damage the fracture surfaces and cause measurement error.

In addition, what a video extensometer does is determining the elongation d_1 (distance between A' and B') at the instance at which the fracture took place. The difference between d_1 and d_0 gives a more realistic measurement of the actual elongation δ. Therefore, if two respective reference points are marked on a line parallel to the longitudinal direction of the sample, the total distances of each point from its respective edge of the fractured surface is the rupture displacement of the sample. Also, the indentation of more pair marks on a sample, along with the calculation of an average rupture displacement by this method, lead to a more accurate and precise measurement of the elongation.

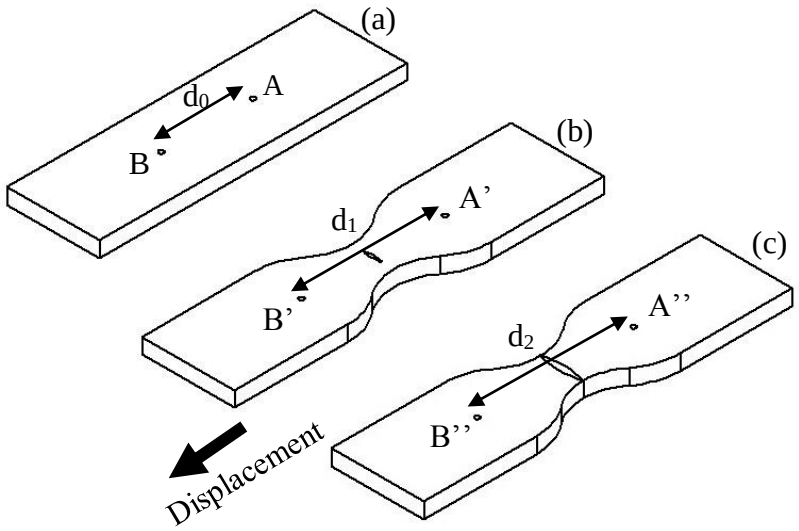

Figure 3-2 : Different elongation stages during a tensile test. (a) Reference points before application of strain. (b) Sample at rupture instant. (c) Sample after rupture

3.3.2 Control and monitoring system

A successful hot ductility test should result in plotting hot ductility curves with high precision and low dispersion. Testing procedures of this kind of experiment are basically fast and last no longer than a few seconds [33]. Thus, the involved instrumentation devices in a hot ductility testing system must exhibit enough sampling rate. This is also essential for the actuators to react as fast as possible.

The fast and relatively complex testing procedure requires a control unit to communicate with other equipment used in the measurement process. This is to receive and analyze data from instrumentation devices and run actuators at the right time. In addition, if the LabVIEW software is applied for programing, it is recommended to select a controller which can be connected to USB ports on laptop computers.

3.4 Conclusion

In order to design the hot ductility testing system, a systematic approach presented in Table 3-4 was conducted. This procedure was followed by an analysis of the possible solutions through studying and identifying the advantages and disadvantages of each solution as well as their side effects on the entire testing system.

Table 3-4 : Procedure followed to design the hot ductility testing system

General Objective	**Related problems**	**Required equipment**	**Possible solutions**
Simulating actual welding condition	Thermal cycle simulation	Heater	IRH, DRH, IH*
		Thermometer	Thermocouples, Infrared thermometers*
	Crack simulation	Mechanical tester	Tensile testing machine*, testing jig
Local determination of weldability	Local determination of ductility	Extensometer	Stroke transducer, clip-on, laser and video extensometer*
	Local application of heat	Cooler	Cooling by grips, air* or water
Automatically controlling the testing procedure	Fast communicating control unit	Controller	USB Portable* and PC non-portable controllers
	Controllable devices	Heater, thermometer, mechanical tester, extensometer	digital or analog I/O (trigger or communication)

*Selected items being applied in the hot ductility testing system.

Finally, the best devices that can effectively function in the system were selected: the induction heating system as the heater, the tensile testing machine for mechanical testing, the use of reference points to measure local length changes and a USB controller to manage the entire testing procedure.

Figure 3-3 shows general arrangement of the mentioned components and devices which can be gathered in the system to conduct a hot ductility test. The welded area in the middle of the sample is surrounded by an induction coil to ensure that the heat will be concentrated in the weld. The infrared lens measures the temperature while it is continually sending the temperature signals to the controller. The sample is fixed between two head of a tensile machine to be fractured at any target temperature. The high speed camera can be used to determine failure temperature which is required for the NST test and will be explained in the next chapter. Besides, fracture elongation of samples which is required to plot the hot ductility curves can be determined by the reference point displacement method.

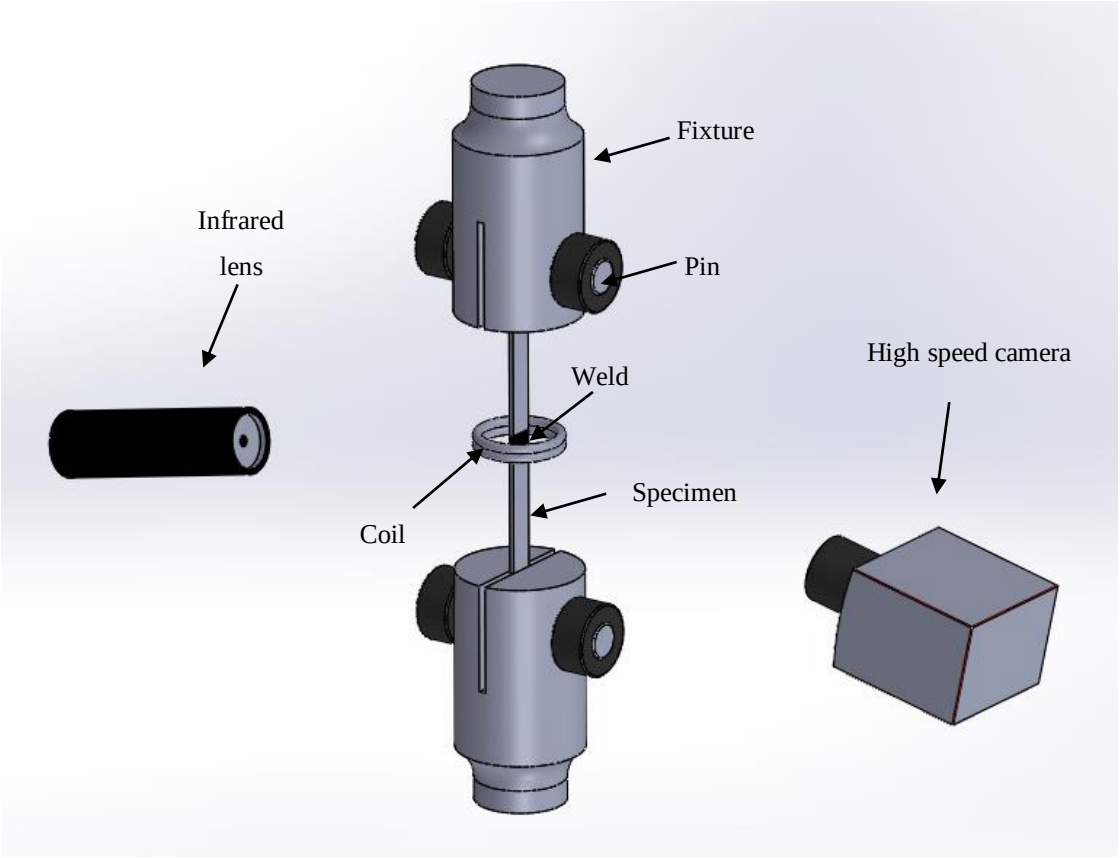

Figure 3-3 : General configuration of the system

CHAPTER 4 EXPERIMENTAL SETUP AND PROCEDURE

The previous chapter resulted in the selection of the equipment and devices that were chosen to be used in the hot ductility testing system. In this chapter, more detailed features and specifications of each device will be reported. Then it will be discussed how it is possible to connect the devices and equipment to setup the system. The explanation of the testing procedure through which the performance of the testing system was evaluated will then be tackled.

4.1 Testing equipment

Based on the analysis of the components qualified to be used in the hot ductility testing system, specifications on each selected piece of equipment and device will be reported in this section.

4.1.1 Induction heater

The induction heating machine used for heating the samples is shown in Figure 4-1. This machine can heat up the samples by generating an electromagnetic force field which produces an electrical current in the samples. The resistance of the material to the electric current then generates heat in the sample.

This machine consists of a power supply, a high frequency output station and a heating coil. The output station is connected to the power supply using a flexible power cable allowing it to be located separately from the power supply [38].

4.1.1.1 Power Supply

The power supply shown in Figure 4-1 is the primary component of the system. Its function is to convert 50/60Hz line power to a high frequency out-put and to deliver this power to the heating coil and the specimen. The Heat Station 2500RHFC operates at a maximum power level of 2500 watts on 208-240V 50/60Hz single phase power. The power supply can operate at variable frequencies which can be adjusted manually. The actual operating frequency is also dependent on the design of the heating coil and on the load inside the coil [38].

Figure 4-1 : Induction heater system including a power supply and an output station [38]

4.1.1.2 Output Station

The output transformer is used to match the heating coil and load to the power supply (Figure 4-1). It is connected to the power supply via a flexible cable which allows the output station and heating coil to be located separately from the power supply [38].

4.1.1.3 Heating Coils

The heating coil is used to concentrate the high frequency magnetic field around the work piece. The coils are constructed from copper tubing and are cooled with water during use. The water cooling is necessary because the high amperage output of the power supply and transformer would cause the coils to heat up very rapidly without proper cooling [38].

The heater is capable to heat thin samples of less than 2mm thick and 20mm width at rates between 60 to 300 ºC/s. The range is approximate and may change depending on different sample geometries and materials. The induction coil of the system consists of two turns of 2mm diameter copper tubing. This helps to localize the heat in the welded area.

4.1.2 Mechanical tester

The mechanical testing of samples was performed on a servo-electrical Instron testing machine, model 1362. The maximum capacity of the machine is of 100kN with a maximum stroke of 100mm. The machine can mechanically test samples at various displacement rates.

The Instron servo-hydraulic machine comes with an 8800 controller, which allows full control over the test instrument and associated devices and enables the recording and processing of the system's

test data. The controller is equipped with a standard computer interface or a Key Panel as a means of system control. In order to control the system with a computer interface, a Wavemaker software is installed on the computer to carry out all of the set-up and control functions with a sampling frequency of 5Hz. For cases where the machine has to be triggered through external signals, the digital input and output port is located on the controller.

4.1.3 High speed camera

In this research, a high-speed recording camera as the one shown in Figure 4-2 is used in NST tests. This device can continuously record and store rapidly moving processes at up to 1,000 images per second (1280(H) x 1024(V) resolution). However, this is increasable to an impression of 93,000 fps with the reduction of the targeted region. In addition, the recording sequence can be started by applying an external trigger signal through the input/output port. This will be further explained in the controlling process of the system [43].

Figure 4-2 : High speed camera [43]

4.1.4 Infrared pyrometer

To measure the heating and cooling temperatures of the samples, a high response speed fiber optic infrared transmitter was used (Figure 4-3). The device, which is from the OS4000 series, can measure temperatures ranging from 350ºC (212ºF) to 1600ºC (2912ºF) using a Fiber Optic Lens Probe [41]. Underneath are listed some of the other specifications of this thermometer:

- Power: 15 to 24 Vdc
- Accuracy: 1% of rdg
- Emissivity: 0.05 to 0.99 adjustable
- Time Constant : 1 msec

Figure 4-3 : High speed fiber optic infrared transmitter with the lens probe [41]

4.1.5 Control system

A NI USB-6210 data acquisition system (DAQ) was used in order to control various instruments and equipment during the measurement process (Figure 4-4). This device can deliver high-speed data streams in portable form through a laptop's USB port. The controller on the Digital I/O side consists of four input-only channels, four output-only channels, a maximum input range of 0-5.25V, a maximum output range of 0-3.8V and a current drive signal of 16mA. Besides, in its Analog Input side, there are eight differential channels with sampling rates of 250kS/s, a voltage range from -10 to 10V and a minimum voltage range sensitivity of 4.8 µV [44].

Figure 4-4 : NI USB-6210 data acquisition system [44]

4.2 Experimental procedure

This section contains the testing procedure followed to evaluate the hot ductility testing system. For this purpose, AISI 1005 grade steel samples were selected to determine preliminary specification of the system such as its precision and its general capability to conduct a hot ductility test. Inconel 718 samples were also used to examine the functionality of the designed system at different stages of a hot ductility test. Finally, the sensitivity of the system was examined by quantifying the SCS of two weld microstructures.

4.2.1 Test specimen

To evaluate the performance of the hot ductility testing system, the following capabilities should be examined:

1- Results precision in hot ductility measurement and NST tests.

2- System's capability to measure the weldability of different microstructures. In this step, pre-welded samples with different weld microstructures were tested.

Keeping this in mind, two types of samples were prepared. For the first step, steel made samples were machined into the standard geometry required for the hot tensile testing procedure shown in Figure 4-5. The chemical composition of the AISI 1005 carbon steel is also outlined in Table 4-1.

For the next step, a semi-automated GTAW welding machine with a filler material was used to make a fully penetrated butt weld joint for Inconel 718 samples. The chemical composition of the samples is presented in

Table 4-3. Two different welds (teardrop and elliptical pool shapes) were produced using different welding parameters reported in Table 4-2. The welding parameters can prompt two weld microstructures with different mechanical properties. The samples were tested with the designed system to evaluate its capability to quantify the SCS of different weld microstructures.

Table 4-1 : Chemical composition of AISI 1005 grade steel (weight %)

Element	**C**	**Si**	**Mn**	**P**	**S**
Chemical composition	0.05	0.04	0.27	0.008	0.008

Table 4-2 : Nominal welding parameters of two types of welds

Weld type	DC Current (A)	Voltage (V)	Welding Speed (mm/s)	Filler wire speed (mm/s)	Diameter of filler wire (mm)	Electrode angle (^{o})
elliptical	44	7	2.55	3.39	0.889	45
Teardrop	69.4	7.4	5.27	5.27	0.889	45

Table 4-3 : Chemical composition of nickel superalloy IN718 (weight %)

Element	Ni	Cr	Nb	Mo	Ti	Al	Co	Mn	Si	Cu	Ta	C	B
Min.	50.0	17.0	4.75	2.80	0.65	0.20							
Max.	55.0	21.0	5.50	3.30	1.15	0.80	1.00	0.35	0.35	0.30	0.05	.08	.006

For mechanical testing, the welded plates were machined into the same geometry as the steel samples. The dimensions in Figure 4-5 were selected to be as close as possible to the recommended sample geometry for the hot tensile test in ASTM, E21 [45]. However, due to some limitations such as the induction coils diameter and the possibility of overheating the grips, a series of modifications were applied to the final dimensions of the samples.

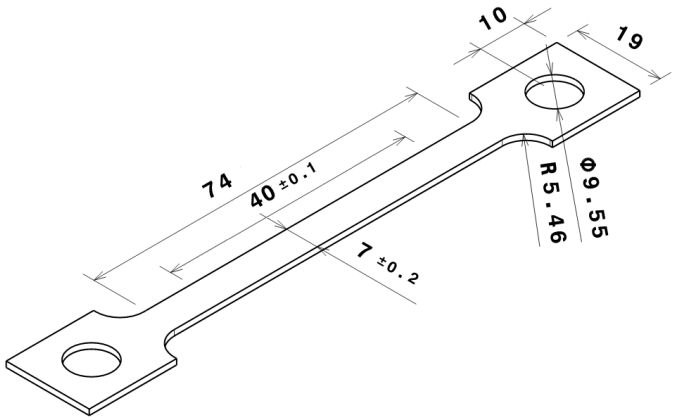

Figure 4-5 : Geometry of the testing specimen (dimensions in mm)

After a visual inspection of the weld quality on the IN718 plates shown in Figure 4-6, the welds with no defects were selected and the specimens were machined to locate the weld in the center of

the specimens (Figure 4-7). The specimens for the final test were machined from the plates and then polished, as shown in Figure 4-8 (a) and (b).

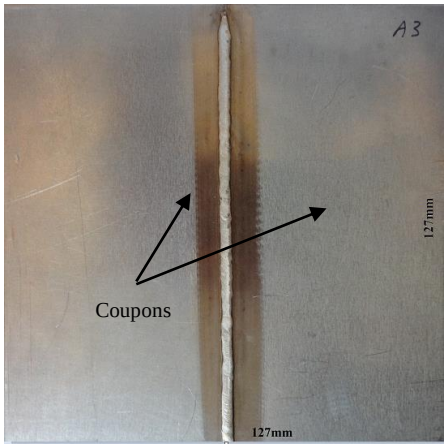

Figure 4-6 : An IN718 plate made from welded coupons

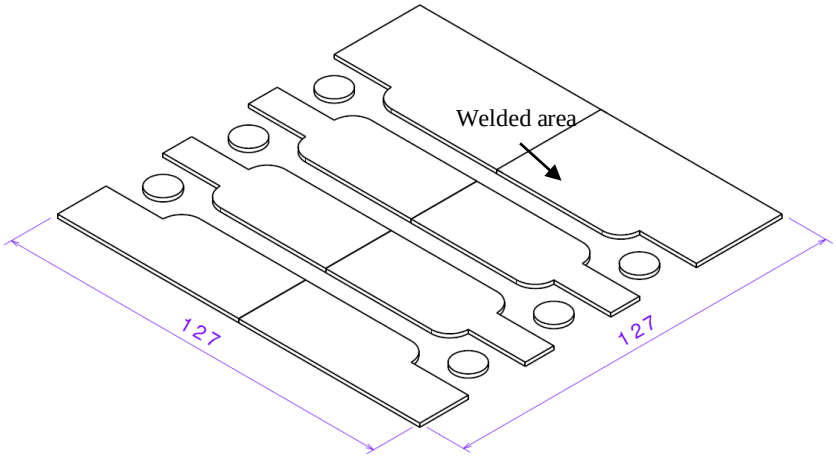

Figure 4-7 : Schematic of the welded plates after machining

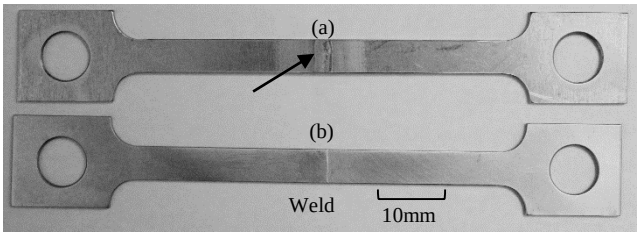

Figure 4-8 : Machined samples : (a) sample with a weld in the center, (b) sample after polishing

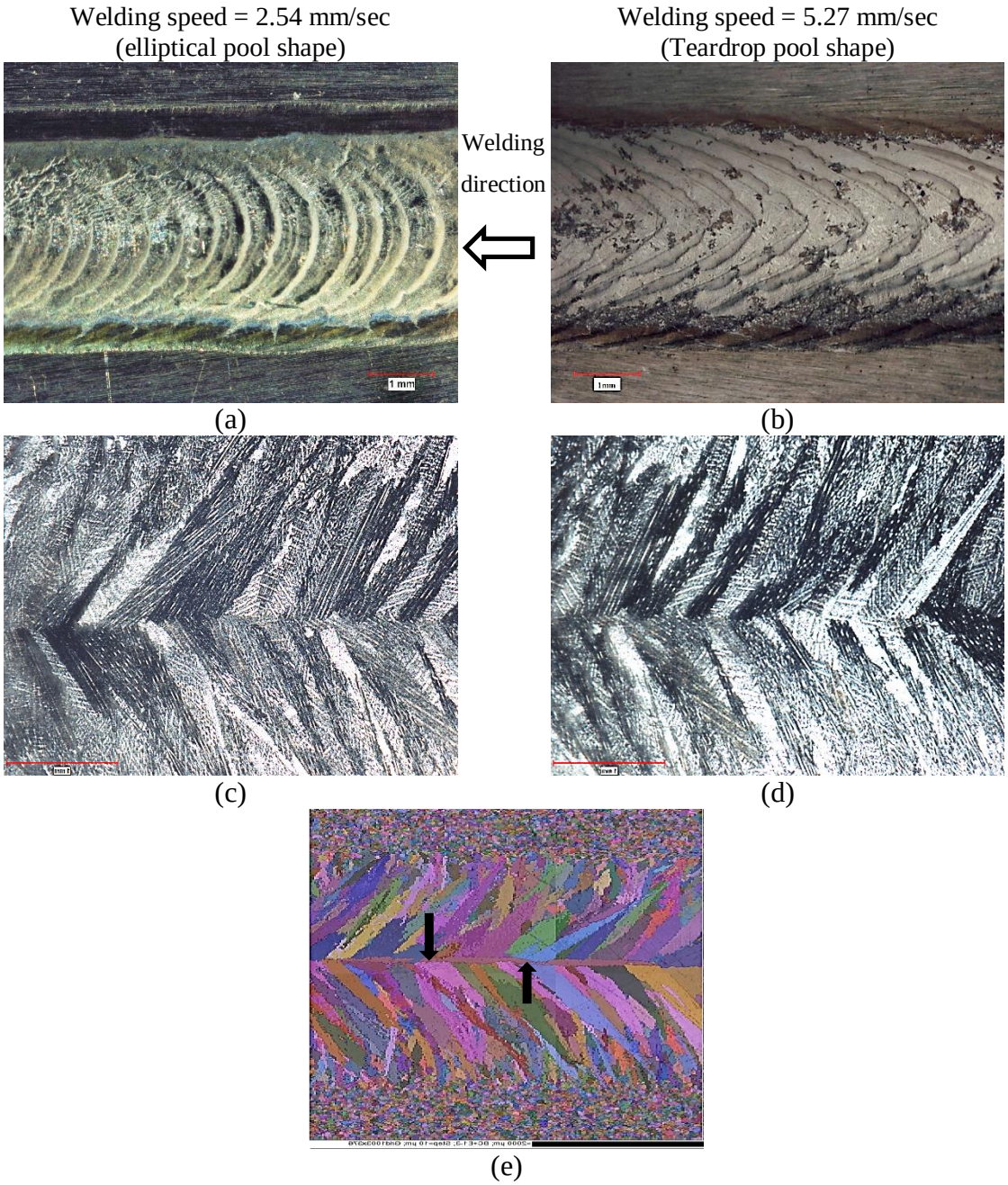

Figure 4-9 : Weld pool shapes (a and b) and the microstructures (c and d) resulted from different welding speeds. Presence of longitudinal center line grain boundary shown by the arrows (EBSD analysis) (e)

Macro pictures and microstructures of the welds are also presented in Figure 4-9 (a), (b), (c) and (d). Figure 4-9 (a) indicates the elliptical pool shape obtained at a lower welding speed. Figure 4-9 (e) shows presence of longitudinal grains at the centerline grain boundaries occurred at the lower

welding speed. Figure 4-10 (a) and (b) presents the observation of the weld microstructures after they experienced the actual testing thermal cycle.

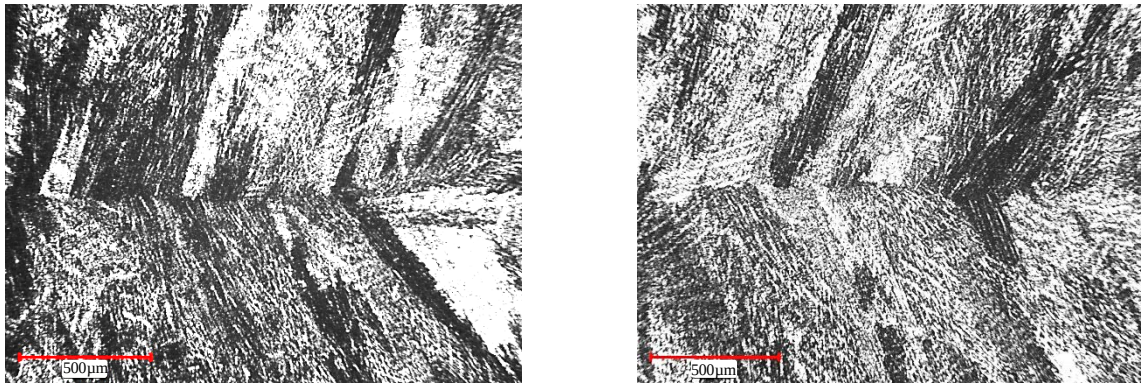

(a) (b)

Figure 4-10 : Microstructures of the welds after experiencing the testing heating cycle, (a) elliptical and (b) teardrop weld pool shapes

4.2.2 System setup and connections

Figure 4-11 shows location, orientation and distances of the induction coil, the infrared lens and the camera in relation to the specimen. The orientations were adjusted so that the camera and the thermometer focus on the center of the welded region. The final setup of the testing system is shown in Figure 4-12.

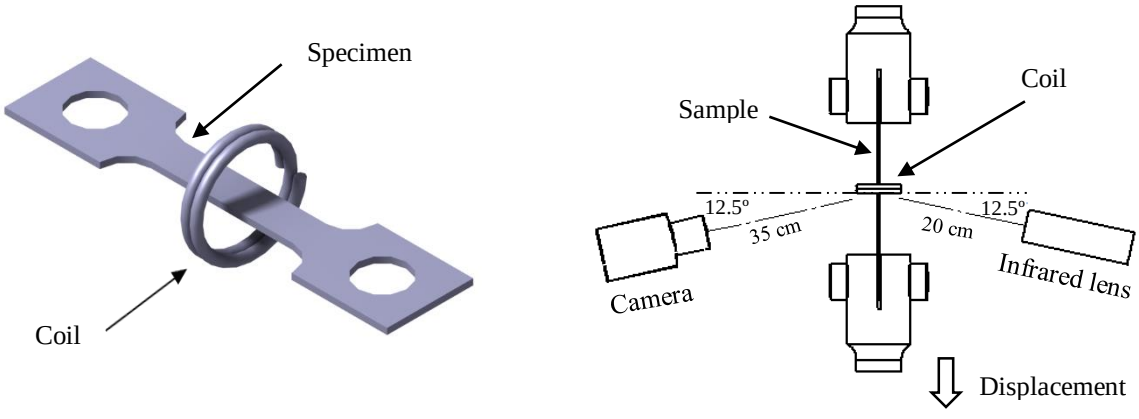

(a) (b)

Figure 4-11 : (a) Coil and specimen. (b) Orientation and distance of the infrared lens and camera relative to the welded region in the specimen

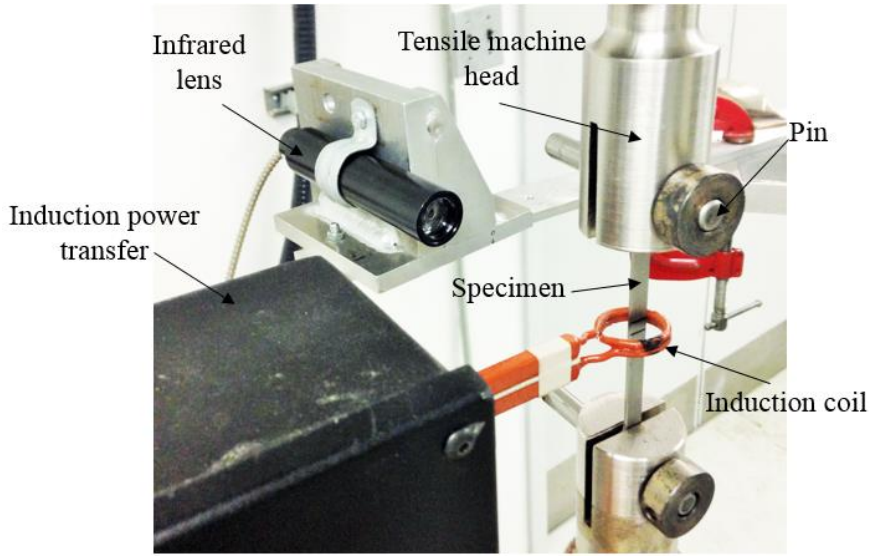

Figure 4-12 : Location of different equipment and devices in the system setup

4.2.3 Coil design

Two important parameters that should be considered in the coil design are the space between the part and the inside diameter of the coil (D_i) as well as the number of tubes (Figure 4-13). If the purpose of the study is to determine the weldability of different weld microstructures, induction coils must concentrate the energy and heat in the weld. Therefore, the welding's width is the first limitation factor for the coil design. The water flow rate in the coil is the other issue that should be taken into account since there should be enough flow to provide adequate cooling in the heated in-service coil. Based on this concept, the number of coil turns can be calculated as follows:

If $S = \pi\ \text{mm}^2$ (minimum coil section recommended by heater producer company) and W = 5mm (average weld microstructure width), inside coil tube diameter $d_i = 2mm$ and the maximum number of coil turns would be equal to 2.

Furthermore, depending on the width of sample in reduced section (W_{rc} = 7mm) and head (W_h = 19mm), inside coil diameter (D_i) was decided to be 20mm.

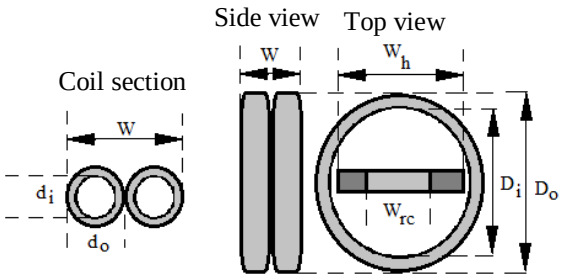

Figure 4-13 : Induction coil geometry with a sample inside

4.2.4 Calibration of the infrared thermometer on LabVIEW

The infrared thermometer used in the testing system was already calibrated by the OMEGA Company with a measurement accuracy and precision of respectively 1% and 0.5% of Rdg. In order to find an equation through which LabVIEW software converts the analog voltage of the thermometer to a temperature, the following procedure was conducted.

The thermometer was set to send a signal at its high alarm to DAQ at every 100°C interval from 400° to 1600°C. It was also simultaneously sending analog voltage to the controller. Then, a LabVIEW program was used to associate the temperatures with the voltages received by DAQ. Afterwards, the driven calibration data was applied to LabVIEW so that the software could show analog output of the thermometer in the form of temperature data.

Since the output digital signal of the thermometer (triggering DAQ system) was not within the working range of the controller, a voltage regulator was used. At this point, an LM78XX series of linear regulators with fixed 5v outputs, manufactured by National Semiconductor Corporation, was employed [46]. Figure 4-14 (a) and Figure 4-14 (b) respectively show the pinout and the general application circuits of the LM78XX voltage regulator. A general connection for calibrating the thermometer is also presented in Figure 4-16 (b).

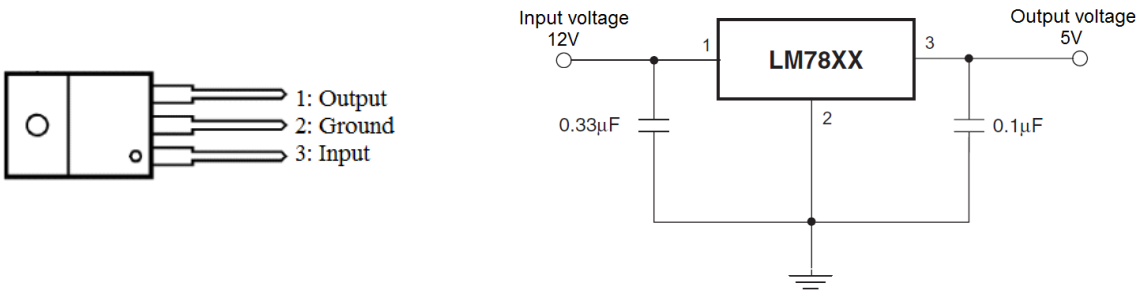

(a) (b)

Figure 4-14 : (a) LM78XX voltage regulator pinout. (b) Application circuits [46]

4.2.5 Measuring and compensating for emissivity

OMEGA provides a large table of emissivity values for common materials at different temperatures. Since emissivity also varies as a function of surface finish and oxidation, it was decided to experimentally measure the emissivity properties of the samples.

The emissivity of the testing material was determined through the contact thermometer method specified in the ASTM standard (E 933-99a) [47]. In this regards, a specimen was heated to a constant temperature that was then simultaneously measured by two thermocouples and by the infrared thermometers. After that, the emissivity gauge on the infrared thermometer was adjusted so that the measured temperature became equivalent to those measured by the other thermocouples.

The hot ductility tests are conducted at different temperature ranges (around melting/solidus temperature). When using an infrared thermometer, emissivity should be determined since it changes with temperature of the material. In order to minimize the effects of the error, the emissivity measurement test was repeated at different temperatures within the range. Finally, the average emissivity obtained at different temperatures was set on the infrared thermometer to be used for on-cooling and on-heating tests.

4.2.6 Heating and cooling rate

The heating rate can be changed by adjusting a power set installed on the heater. Several experiments were conducted to find the power required to achieve the target heating rate of 120ºC/s. During these tests, different samples were heated to 1250ºC and then air cooled. Then, by

using time-temperature data points captured by DAQ, heating and cooling rates were determined and plotted.

4.2.7 Ductility measurement

The elongation of samples after fracture was determined by measuring the difference between reference marks before and after the rupture. A Vickers Hardness machine was used to make diagonal indentations on samples at identical distances (10mm) from the two sides of the welded area shown in Figure 4-15. The rupture displacement at each pair reference points (aȧ, bḃ and cċ) was determined by the sum of the distances from the fractured edge of each mark. The results of this step were then reported in terms of a percentage of elongation using Equation (4-1).

$$\%e = \frac{(d_{ave1} + d_{ave2}) - 10}{10} \times 100 \qquad (4\text{-}1)$$

Where d_{ave1} and d_{ave2} (mm) are the average of three rupture displacement measurements from each side of the fractured surface.

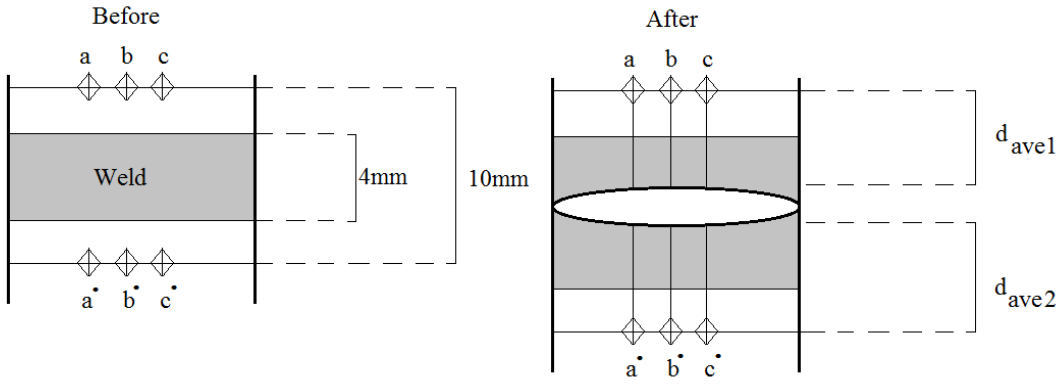

Figure 4-15 : Reference points on a specimen before and after fracture

4.2.8 NST test

NST was determined by rapidly heating the samples with an average heating rate of 120°C/sec while a normal static stress of 3.16 N/mm^2 was applied to the end of the specimen. The temperature at which failure occurred in the sample was reported as NST. The temperature was determined first by the servo-electric controller and then compared with the results obtained using the high recording speed camera.

In order to find the temperature at which the fracture happened, the analog output of the infrared thermometer was connected to the analog input of the tensile machine controller. The machine was then put under load control and, from the recorded load-temperature data, the NST was determined when the load dropped to zero.

The results achieved with this method were compared with the ones gotten by using the high speed camera.

4.2.9 On-heating test

For on-heating tests, the induction heating was transferred to the samples' welded regions through the 5mm-thick and 20mm-diameter coil. Locally heated samples were then pulled to fracture by the servo-electric testing machine at a stroke rate of 10mm/s and a heating rate of 120°C/s. Samples were then tested from about 200°C lower than NST to the point at which ductility dropped to zero. Figure 4-16 shows connections between different devices of measurement to determine the on-heating curve.

For this test, the samples were fixed between the heads of the servo-electric tensile testing machine (Figure 4-12). The location of the samples in the coil was adjusted in a way that the coil surrounded the welded region. Then, the testing machine was set on its displacement-control mode with a 10mm/s displacement rate. A target temperature was then defined in the LabVIEW program. The following steps were conducted automatically through the programmed controller of the LabVIEW software.

1. Trigger the induction heater machine and capture the temperature data from the thermometer.
2. Once the target temperature is reached, a signal from DAQ triggered the tensile machine to pull the sample and stop the heater at the same time.

Fractured samples were observed under microscope to measure the displacement of the indented Vickers marks after the fracture. The results were then used to determine ductility of the materials at various temperatures.

4.2.10 On-cooling test

For the on-cooling test, IN718 samples were heated at a heating rate of 120°C/s and up to 30ºC above NST, then cooled in air. Once the target temperature was reached, the samples were pulled to fail at a constant displacement rate of 10mm/s. The elongation at rupture was then measured with the displacement of the reference points indented at the two ends of the welding area, in the middle of the sample. This procedure was repeated for different samples at every 25°C interval.

The following procedure also shows the steps that were necessary to conduct the test after the samples had been fixed between the heads of the tensile testing machine.

1. Trigger the induction heater machine and heat the sample to above NST.
2. Shut down the heater and wait for the sample to get colder.
3. Once the target temperature is reached, the tensile testing machine is triggered to fracture the sample.

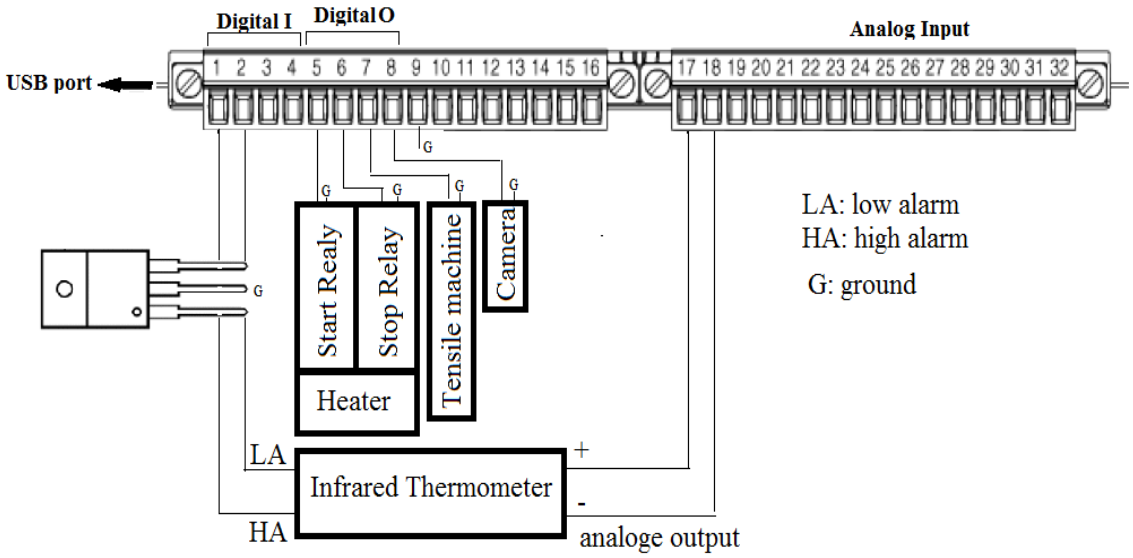

Figure 4-16 : General connection between controller and other devices in the system

CHAPTER 5 RESULTS AND DISCUSSION

This chapter outlines the results achieved from the experimental process to evaluate the hot ductility testing system. The evaluation process carried out by assessing the capability of the system to produce hot ductility testing parameters, determine weldability and quantify the SCS of the weld microstructures. Finally, the system is analyzed in terms of the invested budget and the total testing time.

5.1 Hot ductility testing parameters

This section presents the results obtained from testing the capability of the system to produce the required thermal cycle and to precisely measure ductility.

5.1.1 Thermal cycle

The infrared thermometer and the heater were tested to ensure that the system is capable of producing the required heating cycle. The results will be reported in this section.

For the infrared thermometer, the calibration equation used to relate the output voltage of the thermometer to a temperature was driven from the voltage-temperature relationship presented in Figure 5-1. The equation was put into the LabVIEW program used in the USB DAQ, as well as into the Wavemaker software program of the servo-electric tensile testing machine.

Since the calibration tests were conducted at an emissivity of 0.99, further experiments were required to determine the material emissivity at different testing temperatures. Based on the results presented in Figure 5-2, different emissivity values were used for different temperature ranges as presented in Table 5-1.

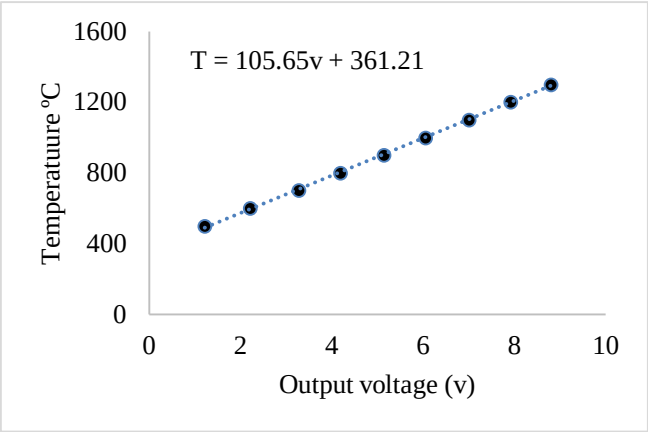

Figure 5-1 : Voltage-temperature relationship of the thermometer at 0.99 emissivity

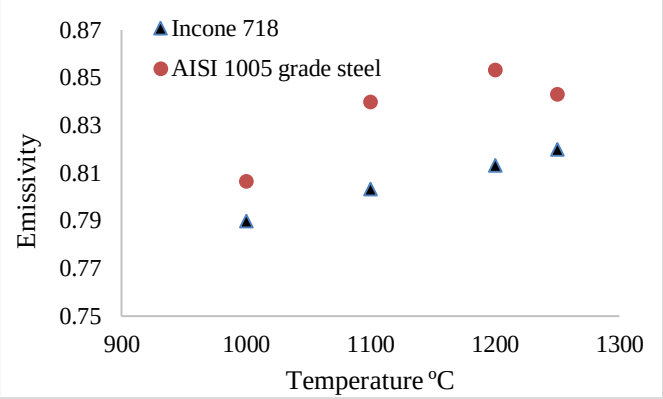

Figure 5-2 : Emissivity of steel 1005 and IN718 samples at different temperatures

Table 5-1 : Emissivity values at various temperature ranges

Temperature range ºC	Emissivity	
	IN718	Steel
1000-1100	0.80	0.82
1100-1200	0.81	0.85
1200-1250	0.82	0.85

In a study conducted by Greene et al [48] the emissivity of oxidized Inconel 718 was measured over the temperature range from 200°C to 1000°C. Their results showed the emissivity increased with the temperature from 0.85 to 0.90.

Furthermore, three tests were conducted to find an average heating rate applied to samples which was 120 ± 4 ºC/s. The cooling rate of the samples after cooling in air was 60ºC/s.

5.2 Testing precision

The precision of the system was measured by the procedure explained in chapter 4. Table 5-2 presents the elongation percentage of the steel samples measured at the same temperature for three repetitions. In the table, precision is expressed in terms of standard deviation (SD). Based on this, the highest deviation was experienced at 1210ºC where the standard deviation was 6 for elongation measurement. There is no detailed study about testing precision of ductility measurements by other researchers. So, the purpose of reporting the SDs is to determine what was the precision at which the hot ductility tests conducted by this system. Similar tests were also conducted to determine the error that occurred during the NST measurement procedure. The standard deviation of the NST tests after three repetitions was 2.10. Figure 5-3 presents the images captured by the high speed camera. The average NST measured by this method was 1405±6ºC which confirms accuracy of the results obtained by the tensile testing machine.

Table 5-2 : Testing repetitions for the on-heating and NST tests

Temperature, ºC	**Elongation %**			**Average**	**SD**
	1	**2**	**3**		
1340	1.2	3.0	0	1.4	1.5
1330	8.1	9.1	7.0	8.0	1.0
1210	42.1	48.9	36.8	42.6	6.0
NST	**Temperature, ºC**			1410.2	2.1
	1412	1407.9	1410.8		

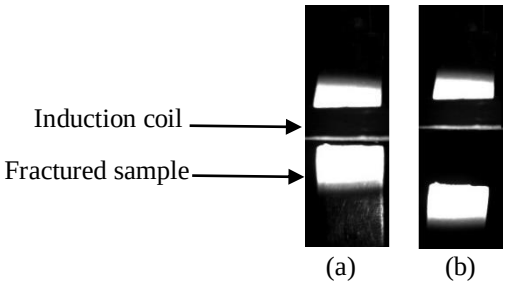

Figure 5-3 : Images of a fractured sample during an NST test, captured by the high speed camera. (a) Fracture just occurred at 1405ºC, (b) An image captured within a few millisecond after the fracture.

5.3 Weldability test

In order to evaluate the capability of the system to quantify the weldability, hot ductility tests were conducted on steel and IN718 samples. First, steel samples were tested to see if the desired curve and parameters could be achieved. The IN718 test results were then used to plot hot ductility curves which can be used to quantify the weldability.

5.3.1 Hot-ductility behavior of steel samples

AISI 1005 grade specimens were used to obtain the ductility behavior of the alloy within the range between 1000 and 1500ºC. The other goal of the test was to measure nil strength and nil ductility temperatures.

Distance between reference point at rupture *(d)* and the elongation percentage *(%e)* of steel specimens were measured at different temperatures and are reported in Table 5-3. The table also presents the NST test results of the steel samples at three repetitions where the rupture elongation remained unchanged. Fractured specimens at various temperatures are presented in Figure 5-4. The figure shows how ductility changed at different temperatures. The on-heating data points of the steel samples at various temperatures are presented in Figure 5-5. Equation (5-1) can be used to show the relationship between the elongation percentage (*e%*) and temperature (*T*).

$$e\% = -0.001T^2 + 2.1883T - 1197.8 \ (R^2=0.92) \qquad (5\text{-}1)$$

Various measurements at smaller temperature intervals were conducted while the ductility of the samples quickly dropped to zero. Measurements at smaller intervals made it possible to determine the nil ductility temperature of AISI 1005 steel, which is about 1350ºC.

Table 5-3 : Rupture elongation percentage of steel samples at different heating cycles

Heat cycle	Temperature (ºC)	d (mm)	e%
On-heating	1070	14.518	45.1
On-heating	1110	13.830	38.3
On-heating	1150	14.414	44.1
On-heating	1190	13.521	35.2
On-heating	1210	14.214	42.1
On-heating	1230	13.842	38.4
On-heating	1250	13.132	31.3
On-heating	1290	13.201	32.0
On-heating	1310	11.012	10.1
On-heating	1330	10.812	8.1
On-heating	1340	10.121	1.2
On-heating	1350	10	0
NST	1412	10	0
NST	1407.9	10	0
NST	1410.8	10	0

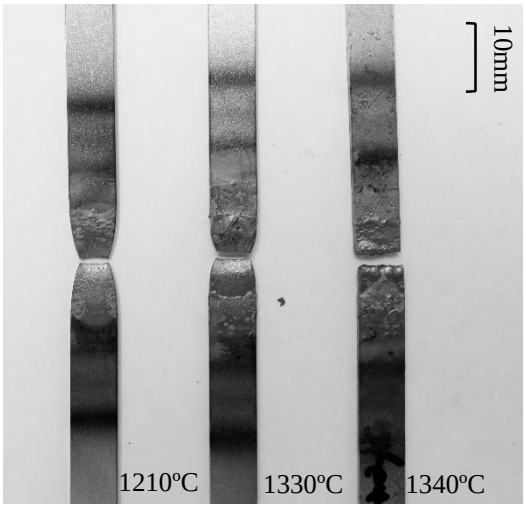

Figure 5-4 : Fractured steel samples in the on-heating tests

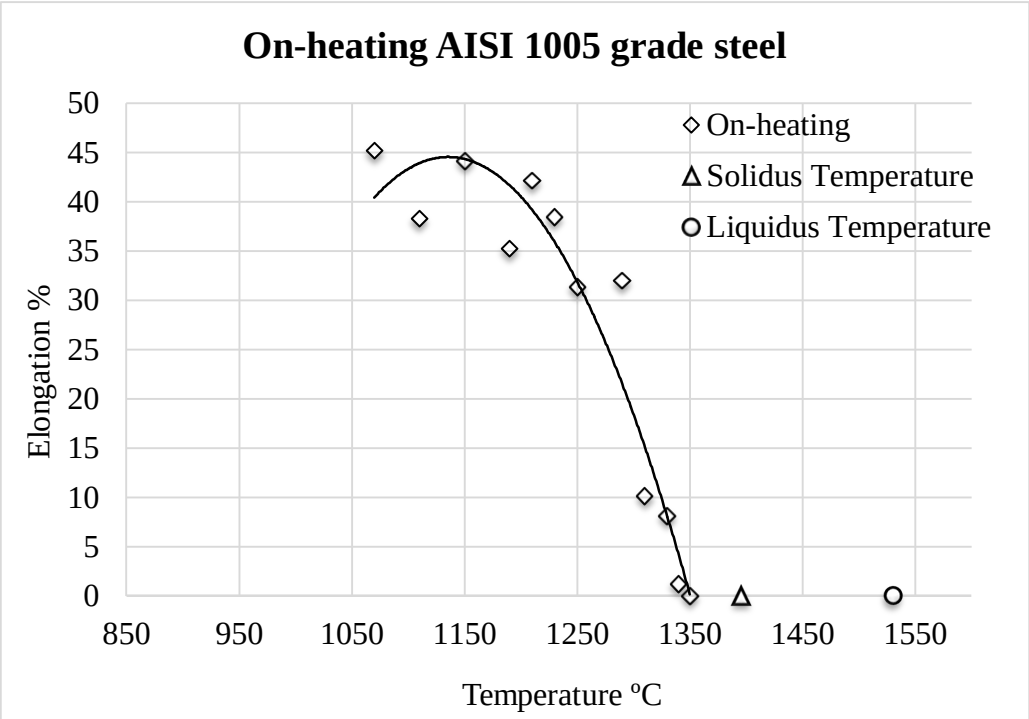

Figure 5-5 : On-heating curve of AISI 1005 grade steel

Based on the phase diagram Fe-C, solidus and liquidus temperatures of 1005 grade steel are about 1400 and 1536 ºC, respectively. The results show that the steel lost its ductility 50 ºC below the solidus temperature. This loss in ductility is similar to the findings of other researchers conducting hot ductility tests on other materials [6, 32, 36, 40]. The results also showed that the average NST of the steel specimens is about 1410 ºC which is a little more than the solidus temperature. One possible reason for this difference may be the high heating rate that the specimens experienced during the NST test, compared to the equilibrium phase diagram which is used for low heating rates. At higher heating rates, the steel will stay in a solid state for longer when the measured NST is above the liquid state.

5.3.2 Hot ductility of Inconel 718 weld microstructures

In the first step, the NSTs of Inconel 718 welds (elliptical and teardrop pool shape welds) were measured using the procedure discussed in chapter 4. The measured NSTs for the two weld microstructures are presented in Table 5-4. The mean NST values for elliptical and teardrop pool shape welds are 1231.5±4.8 and 1236.3±6.2ºC, respectively.

Table 5-4 : NST results for microstructures of two welding pools

NST (ºC)	Repetition			Average	SD
	1	2	3		
Elliptical	1233.2	1235.3	1226.1	1231.5	4.8
Teardrop	1242.5	1236.3	1230.1	1236.3	6.2

The on-heating and on-cooling elongation percentage for the weld pool shapes are shown in Table 5-5. For on-heating tests, the table presents the target temperatures at which samples were pulled until fracture occurred. Peak temperatures of on-cooling test was chosen to be 30ºC above nil strength temperature.

Figure 5-6 shows the fractured specimens over hot ductility tests. The order of specimens shows how ductility decreased at various temperature. Hot ductility curves of two microstructures are also presented in Figure 5-7 and Figure 5-8.

Table 5-5 : Rupture elongation percentage of IN718 welds at different heating cycles

Heat cycle	**Peak temperature ºC**		**Target temperature ºC**	**Rupture elongation %**	
	Elliptical	Teardrop		**Elliptical**	**Teardrop**
On-heating	1050	1050	1050	26.8	26.1
On-heating	1075	1075	1075	26.2	24.5
On-heating	1100	1100	1100	26.6	26.8
On-heating	1150	1150	1150	10.3	14.0
On-heating	1175	1175	1175	0	0
On-cooling	1261	1269	1050	0	0
On-cooling	1261	1269	1025	3	0
On-cooling	1261	1269	1000	7.4	21.3
On-cooling	1261	1269	975	21.3	24.2
On-cooling	1261	1269	950	24.5	22.6

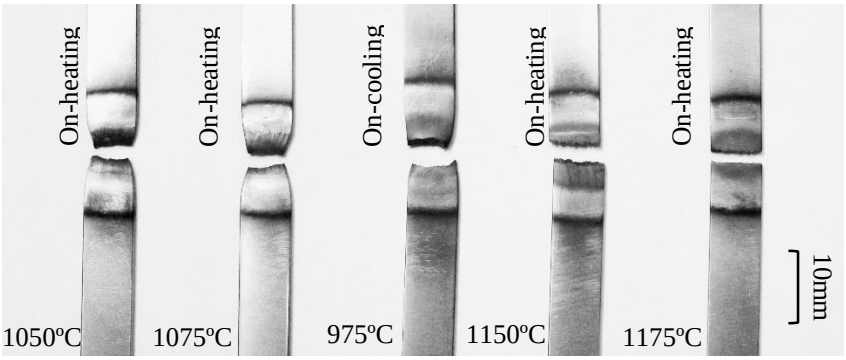

Figure 5-6 : Fractured specimen of IN 718 samples during hot ductility test

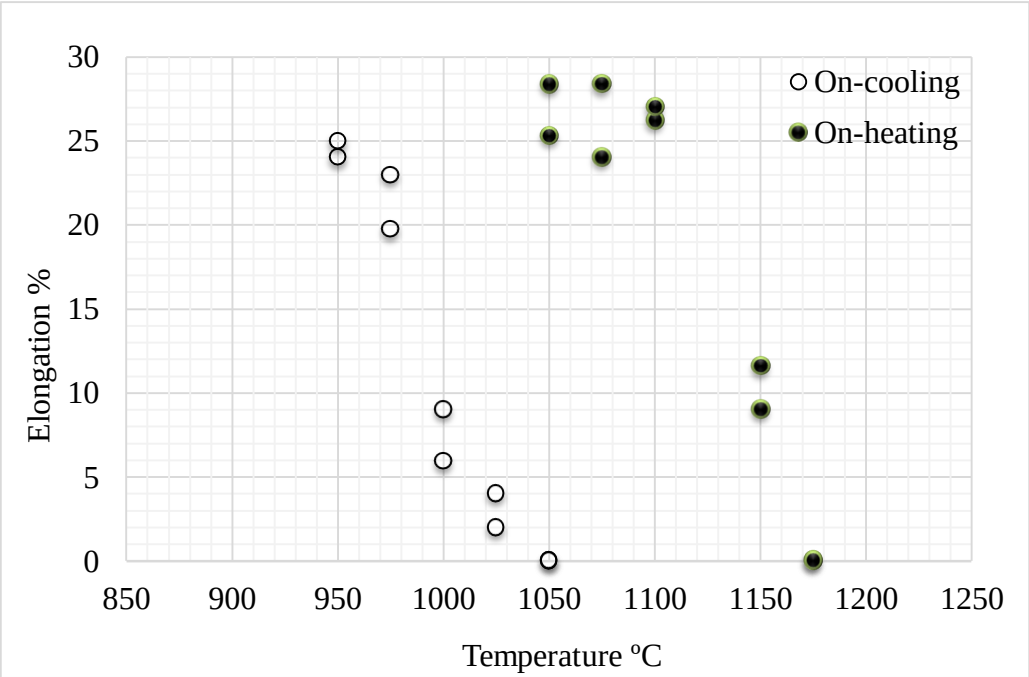

Figure 5-7 : Hot ductility curves of elliptical pool shape weld

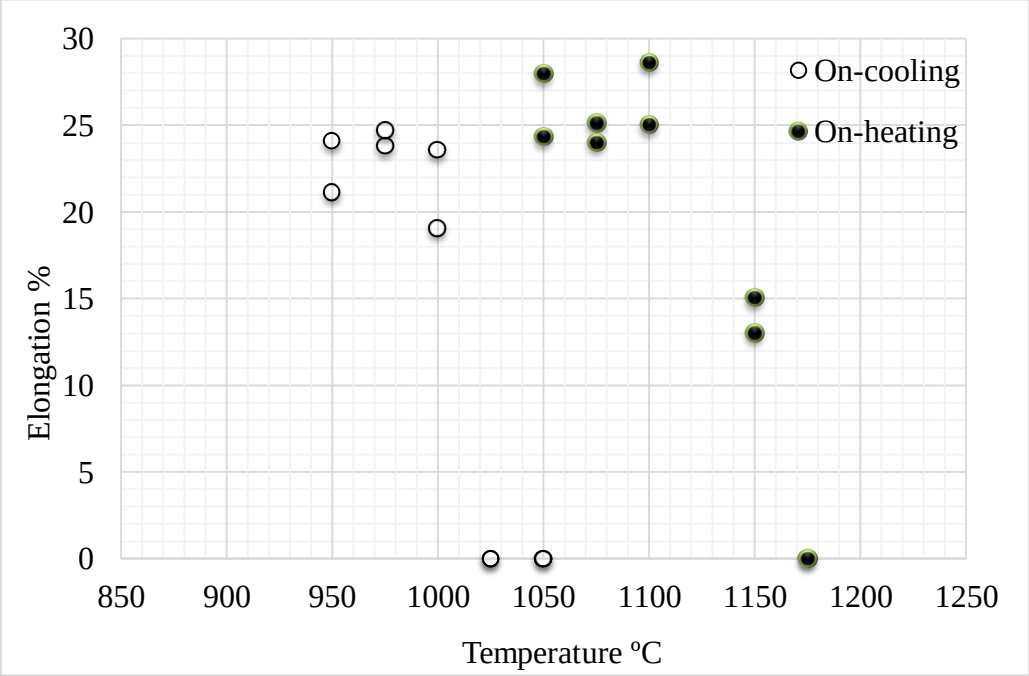

Figure 5-8 : Hot ductility curves of teardrop pool shape weld

The hot ductility behavior of the welds were evaluated based on the on-heating and on-cooling curves. Since the number of available samples were not enough to exactly determine NDT and DRT, these temperatures were reported where the ductility has been restored to 5% [3, 6, 33].

Table 5-6 presents hot ductility parameters of the current research and those determined by other researches using a Gleeble machine.

Table 5-6 : Comparison of hot ductility parameters measured by different researchers

Researchers (material)	Hot ductility parameters, ºC				
	NST	NDT	DRT	BRT	PT
(Elliptical pool shape IN718weld)*	1231	1163	1010	221	1261
(Teardrop pool shape IN718weld)*	1236	1167	1019	217	1269
Quigley [40] (IN718)	1232	1197	1051	181	1232
Knock [6] (IN718)	1245	1194	1051	194	1232
Chhatre [37] (IN718)	1253	1154	1037	216	1232

*Current research

Despite of the fact that geometry of the tested specimens in the current study is different from those tested by other researches, hot ductility parameters are relatively similar. The difference between the results of this study with the findings of other researchers may be explained by the following reasons:

1- Different cross sections of the tested specimens;

   In the hot ductility tests by Gleeble, a 10mm diameter bar is used for hot tensile testing. Whereas, in the current project, samples with rectangular cross section of 7×1.27 mm were tested. Stress concentration on the edge of the rectangular cross section may cause samples to fracture at lower temperatures. Therefore, there would be an underestimation in the NST measurements of this project. This would also be the same case for the results obtained from the NDT and DRT tests. However, for the comparative evaluation of weldability this does not have a significant effect.

2- Different mechanical properties;

In this research IN 718 weld microstructures were tested. Since mechanical properties are closely related to the microstructure, we cannot expect to have identical values.

3- Different peak temperatures;

In all the research, the peak temperatures were chosen to be at or below NST. In the current study, the peak temperature was almost 30 ºC above NST to quantify solidification cracking susceptibility. This can directly affect the results obtained from on-cooling test such as DRT and BTR [3, 32]. When a material experiences higher temperatures, more liquid films will be generated and this decreases the temperature at which ductility recovery occurs.

5.4 Sensitivity to quantify the SCS of the weld microstructures

In order to compare SCS of two weld microstructures different methods are used. For the first method, hot ductility parameters such as NST, NDT, DRT and BRT are used to compare the microstructures. As Figure 5-9 shows, there is no significant difference between the obtained parameter for the two microstructures.

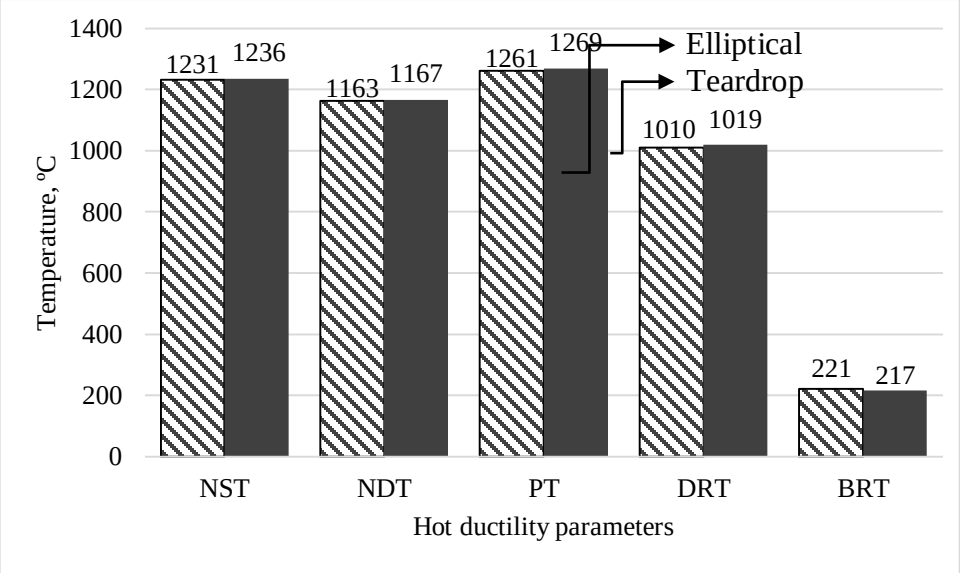

Figure 5-9 : Comparison of the hot ductility parameters for the weld microstructures

These temperatures are often used to interpret the hot ductility testing results, however, further analysis should be carried out on these curves to determine the HCS. In a study conducted by Joel Andersson et al, the hot ductility of several Haynes 282 alloys have been quantified using a Gleeble

machine [36]. The purpose of their research was to investigate how heat treatment would influence the weldability of the alloys.

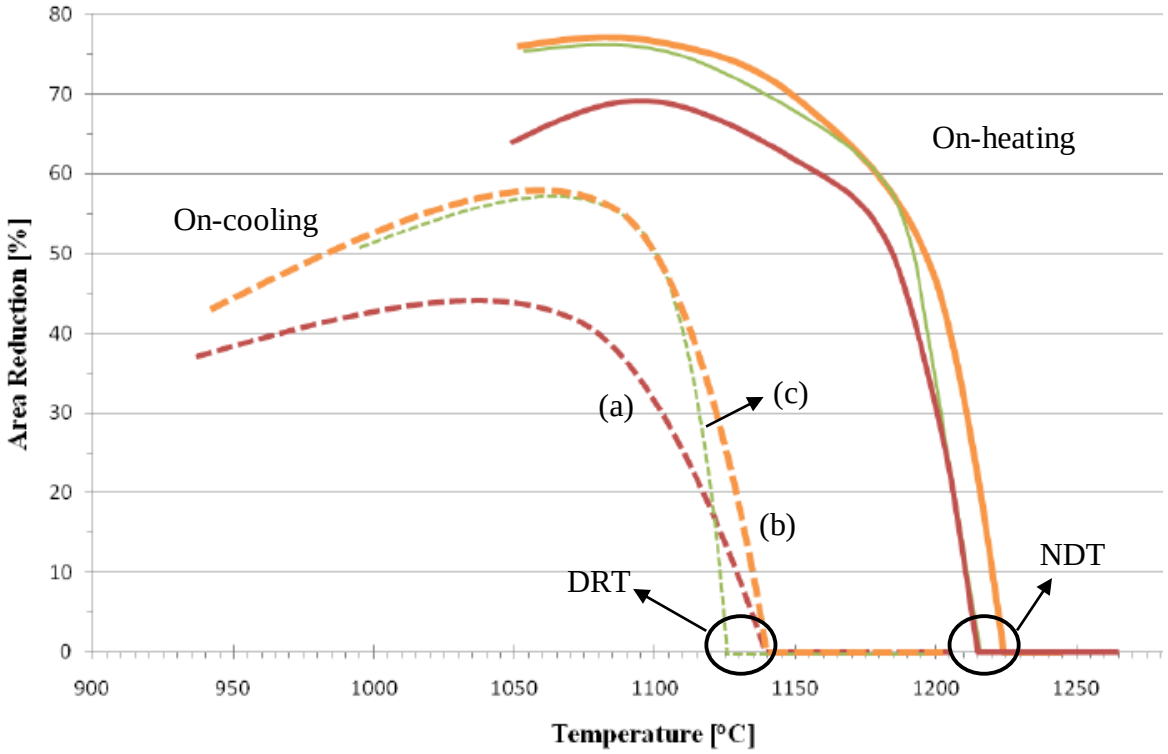

Figure 5-10 : Comparison of the hot ductility for the three Haynes 282 alloys (a, b and c) with the same NST and peak temperatures [36].

As Figure 5-10 shows, Andersson *et al* stated that despite the DRT, NDT, NST and BRT have the same values, these alloys are not necessarily the same in HCS and the alloy a is the most susceptible to form hot cracking.

In the current study, to compare SCS of the two welds, further analysis have to be carried out on the hot ductility curves. Since solidification cracking occurs during weld cooling and not heating, the on-cooling curves are used for the analysis. In addition, the ductility recovery rate can only be measured during on-cooling process. Moreover, measuring the temperature range at which the recovery occurs is one of the best ways to quantify HCS of a material [49].

Figure 5-11 shows on-cooling curves of both welds on the same graph. By observing the curves, it can be determined that the teardrop pool shape is the most resistant to solidification cracks as it recovers its maximum ductility in about half of the temperature compared to the elliptical one. The

ductility recovery temperature ranges for elliptical and teardrop pool shapes are approximately 50 and 100 ºC, respectively.

Furthermore, Figure 5-11 presents ductility recovery lines (DRL) which go through the starting point of each curve until 90% of the maximum ductility is recovered. It can be graphically determined that the teardrop weld DRL is steeper than the other line which means it can recover its ductility faster. The faster the ductility recovers, the less time the material has to form cracks.

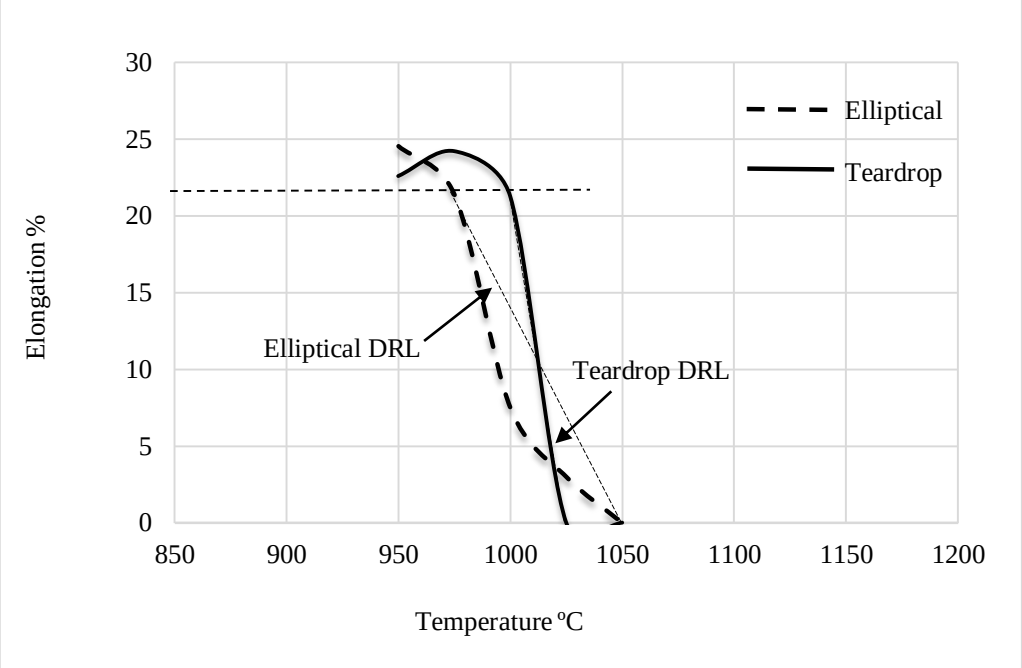

Figure 5-11 : On-cooling curves and the ductility recovery lines (DRL) of two weld microstructures

In a study conducted by Knock, weldability of IN718 and Alloy X were compared. Figure 5-12 presents the on-cooling curves which were used to determine which alloy is more weldable. According to his findings, Inconel 718 is more weldable since it has a faster recovery rate and its ductility recovery temperature is half of the alloy X.

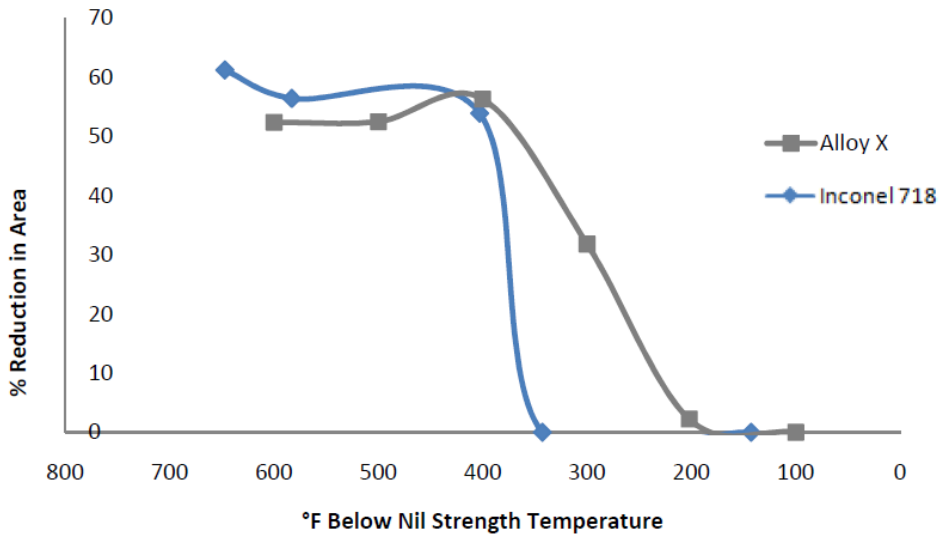

Figure 5-12 : On-cooling curves of IN718 and alloy X [6].

5.5 System analysis

In chapter 2, 3 and 4, design methodology of the hot ductility testing system was described and the equipment with the required specifications were identified. In this process, using the available equipment at the school was preferred as long as they could meet the expected specifications of the test. However, some equipment had to be purchased. Table 5-7 presents the price of each item used in the testing system. For setting up the system, further analysis carried out to determine total testing time including the time required for connecting and adjusting devices and machines, testing samples and final analysis (Table 5-8).

Table 5-7 : Total cost to setup the hot ductility testing system

Equipment	Availability	Price ($)	Model
Heater	No	**9,520**	Magneforce, Heat Station 2500RHFC
Mechanical tester	Yes	-	Servo-electrical Instron testing machine, model 1362
Controller	No	**775**	NI USB-6210
High speed camera[1]	Yes	-	MotionBLITZ, Cube4
Thermometer	No	**2,871**	OMEGA OS4000 series
Indenting reference marks on samples and elongation measurement	Yes	-	Hardness Vickers testing machine
30 testing samples		**2,700**	Standard hot tensile sample for two hot ductility curves.

[1] High speed camera is optional and only used to confirm results obtained from tensile machine

Table 5-8 : Required time at different testing stages to determine weldability of a material

Testing procedure	Required time (h)	Description
System setup and connections	2	This includes the time required for infrared thermometer, induction coil and heating rate calibration and providing connections between different equipment.
Testing samples	2	Testing approximately 30 samples with required installation to heads of tensile machine.
Analysing results	4	Indenting samples for reference marks at the desired location on samples and measuring final rupture displacement under microscope.

Based on the results presented in Table 5-7and Table 5-8 the required budget to setup such a weldability testing system in a mechanical engineering department of École Polytechnique de Montréal is about 50,000 which includes 15,866 $ for testing equipment and materials as well as 34000$ for student financial support. In addition, the total required time to quantify HCS of a material is about 8 hours. The required time for the sample preparation is not considered. It may vary from one week to one month.

The price of a Gleeble machine is at least 500,000$. If the purpose of a research is only to determine the weldability of a material, it is not reasonable to buy one. The developed hot ductility testing system can be setup at a much lower price in laboratories equipped with a tensile testing machine. Individual comparisons between equipment applied in both systems indicates that there is no significant difference between capabilities of each item. The biggest advantage of the Gleeble is its heating system which can provide a more uniform heating profile over the sample. On the other hand, the total testing time by a Gleeble machine is longer. To measure a temperature in a Gleeble machine, thermocouples are recommended which must be welded in the middle of each specimen. This would increase the total testing time of a test.

CONCLUSION

The hot ductility testing system that was designed and developed has met the required specifications of this project. The technical capability of the system was experimentally evaluated, and from that evaluation the following conclusions can be made:

1- The best possible solution to fulfil the required specificities of the system was to use an induction heater for the heating system, a servo-electric tensile machine for mechanical testing, an infrared thermometer for temperature measurement and a portable USB DAQ for controlling the testing procedure and sequences. The hot ductility of the samples was also determined by measuring the displacement of the indented marks before and after the fracture.

2- The thermal cycle produced by the system and used to test the samples was of about 120º ±4 C/s in heating and 60ºC/s in cooling.

3- The final testing precision of the system in terms of maximum standard deviation is 6 on hot ductility measurements.

4- The system is capable to fulfil objectives of the current project. However, the reliability of its measurements can be improved in some aspects which will be explained in the following section.

5- The system is also sensitive enough to detect a weldability variation caused by different weld microstructures.

6- The total testing time to determine the hot ductility parameters of one microstructure with 30 machined samples is about 8 hours.

7- Setting up the system with the specifications mentioned above cost about 16,000 which is within the defined budget by the client.

RECOMMENDATIONS AND FUTURE WORK

The system developed in this project could be improved in some aspects, and they will be explained in this section. These improvements can enhance the repeatability and the reliability of the system as well as reduce its final price. Generally, the errors that occurred at different stages of the testing process altered the final precision and accuracy of the measured values. If these errors are minimized the total testing precision will be increased.

Heating samples with induction heaters is not always perfect in terms of the application of a constant heating rate to the samples. In addition, the heating rate may vary from one test to another even when using the same material and geometries. The heater used in this project has an adjustable power set to control the heating rate. If the power of the heater can be automatically controlled by a control system, more identical heating rates can be achieved during different tests.

Furthermore, there are improvements to be made concerning the test thermal cycle. In this system, samples were cooled in air without any control over the cooling rate. Heating the samples to various peak temperatures can promote numerous cooling rates and would not provide an identical scale to compare the weldability of different materials. Therefore, if the system could be equipped with an additional system to control the cooling rate, a wide range of materials could be tested and compared.

In measuring the rupture elongation, the reference points were not indented exactly at the two ends of the welds, and the elongation of the base metal has also altered the final results. If the points could be protected from melting at high temperatures and were visible after the tests, they could be indented closer to the welds. This would eventually provide more realistic measurements of the welds' ductility.

The servo-electric tensile testing machine is the most expensive equipment used in this testing system. If a testing jig could be designed for mechanical testing processes, the total cost would dramatically drop, particularly for the laboratories that are not equipped with a tensile machine. The jig must have at least the two following capabilities:

- Applying constant loads to the specimens
- Applying constant strain rates to specimens at targeted temperatures

REFERENCES

[1] T. M. Pollock et S. Tin, "Nickel-based superalloys for advanced turbine engines: chemistry, microstructure and properties," vol. 22, n°. 2, p. 361-374, 2006.

[2] K. Shinozaki et al., "Comparison of hot cracking susceptibilities of various Ni-base, heat-resistant superalloys by U-type hot cracking test. Study of laser weldability of Ni-base, heat-resistant superalloys (2nd Report)," vol. 13, n°. 12, p. 952-959, 1999.

[3] J. C. Lippold et al., "Precipitation-strengthened Ni-base alloys," dans *Welding metallurgy and weldability of nickel-base alloys* Hoboken, New Jersey: John Wiley & Sons, 2011, p. 157-249.

[4] M. Brochu et al., "Solidification cracking of IN 718 TIG welds," communication présentée à Beijing, China, 2013.

[5] R. Schafrik et R. Sprague, "Saga of gas turbine materials: Part III," vol. 162, p. 27-30, 2004.

[6] N. O. Knock, "Characterization of Inconel 718: Using Gleeble and Varestraint testing methods to determine the weldability of Inconel 718," Materials Engineering, California Polytechnic State University, San Luis Obispo, 2010.

[7] J. D. Matthew et J. D. Stephen, *Superalloys: a technical guide*, 2e éd. vol. 409. United States of America, Materials Park, OH 44073-0002: ASM international, 2002.

[8] E. Miller. (Jan 2015). *TIG Welding Tips*. [En ligne]. Disponible: http://www.millerwelds.com/resources/tech_tips/TIG_tips/setup.html

[9] (Jan 2015). *Guide to TIG Welding (GTAW)*. [En ligne]. Disponible: http://www.weldguru.com/tig-welding.html

[10] (Jan 2015). *Why Welds Crack*. [En ligne]. Disponible: http://weldinganswers.com/why-welds-crack/

[11] J. R. Davis, *ASM Handbook: Nondestructive evaluation and quality control* vol. 17: ASM International, 1989, p. 582–609.

[12] J. C. Lippold et al., "An investigation of weld metal interfaces," p. 141-146, 1992.

[13] P. Wen et al., "Study on solidification cracking of laser dissimilar welded joints by using in-situ observation and numerical simulation," vol. 54, n°. 9-10, p. R257-R266, 2010.

[14] J. C. Lippold et al., "Weldability Testing," dans *Welding metallurgy and weldability of nickel-base alloys* Hoboken, New Jersey: John Wiley & Sons, 2011, p. 379-402.

[15] B. Alexandrov et al., "Evaluation of weld solidification cracking in Ni-base superalloys using the cast pin tear test," dans *Hot Cracking Phenomena in Welds II*: Springer, 2008, p. 193-213.

[16] W. F. Savage et C. D. Lundin "The Varestraint test," vol. 44, n°. 10, p. 433s – 442s, 1965.

[17] A. Lingenfelter, "Varestraint testing of nickel alloys," p. 430s-436s, 1972.

[18] J. Andersson et al., "Hot cracking of Allvac 718Plus, alloy 718 and Waspaloy at varestraint testing," communication présentée à Winnipeg, Canada, 2008.

[19] T. Pfeifer et al., "Testing of solidification cracking susceptibility of MAG welded overlays on S355JR steel using a Transvarestraint test," p. 5-11, 2013.

[20] Y. Arata et al., "Varestraint test for solidification crack susceptibility in weld metal of austenitic stainless steels," vol. 3, n°. 1, p. 79-88, 1974.

[21] J. Andersson, "Solidification Cracking of Alloy Allvac 718Plus and Alloy 718 at Transvarestraint Testing," communication présentée à Konferensbidrag, övrigt, 2008, p. 157-169.

[22] J. DuPont et al., "Solidification and Weldability Superalloys," p. 417s-431s, 1998.

[23] G. M. Goodwin, "Development of a new hot-cracking test - The sigmajig," vol. 66, n°. 2, p. 33-S-38-S, 1987.

[24] J. Lippold et al., "Sigmajig Weidability Test," p. 81s-92s, 1995.

[25] M. Mossman et J. Lippold, "Weldability testing of dissimilar combinations of 5000-and 6000-series aluminum alloys," vol. 81, n°. 9, p. 188s-194s, 2002.

[26] M. Yamamoto et al., "Study of evaluation method for liquation crack initiation in the HAZ of a laser weldment," vol. 49, n°. 9-10, p. 49-57, 2005.

[27] F. Matsuda et al., "Investigation of weld solidification cracking by MISO technique-2," vol. 6, n°. 3, p. 394-400, 1988.

[28] K. Shinozaki et al., "Effect of grain size on solidification cracking susceptibility of type 347 stainless steel during laser welding," vol. 39, n°. 2, p. 136-138, 2012.

[29] S. H. Song et al., "Tin-induced hot ductility degradation and its suppression by phosphorus for a Cr–Mo low-alloy steel," vol. 595, p. 188-195, 2014.

[30] S. Brown et al., "A 3D numerical model of the temperature-time characteristics of specimens tested on a Gleeble thermomechanical simulator," vol. 5, n°. 6, p. 539-548, 1997.

[31] S. J. Norton, "Development of a Gleeble based test for post weld heat treatment cracking in nickel alloys," Welding Engineering, The Ohio State University, Ohio, USA, 2003.

[32] S. T. Mandziej, "Testing for susceptibility to hot Cracking on Gleeble™ physical simulator," dans *Hot Cracking Phenomena in Welds*, T. Böllinghaus et H. Herold, Édit.: Springer Berlin Heidelberg, 2005, p. 347-376.

[33] "Gleeble Users Training " dans *Gleeble Systems and Applications*, D. S. Inc., Édit., éd. New york: Dynamic Systems Inc. , 2010, p. 377.

[34] G. Pahl et al., *Engineering design: a systematic approach*, 3e éd. Verlag, New York: Springer, 2007.

[35] J. C. M. Farrar, "Hot cracking tests - The route to international standardization," dans *Hot Cracking Phenomena in Welds*, T. Böllinghaus et H. Herold, Édit.: Springer Berlin Heidelberg, 2005, p. 291-304.

[36] J. Andersson et al., "Hot ductility study of HAYNES 282 superalloy," dans *Superalloy 718 and Derivatives*, Hoboken, NJ, USA: John Wiley & Sons, Inc, 2010, p. 538-554.

[37] R. Chhatre, "Weldability and post-weld heat treatment of a novel Ni-based alloy," Material Engineering, California Polytechnic State University, San Luis Obispo, 2006.

[38] "HeatStation 2500RHFC, Induction Heating System," M. Inc., Édit., éd. Warren, OH, 2010.

[39] J. Hooijmans et al., "Effect of multiple postweld heat treatment on the weldability of alloy 718," vol. 718, p. 625-706, 1997.

[40] S. Quigley, "A Quantitative study of the weldability of Inconel 718 using Gleeble and Varestraint test methods," Materials Engineering, California Polytechnic State University, California 2011.

[41] "OS4000 SERIES - High speed fiber optic infrared transmitter," I. Omega Engineering, Édit., éd. United States of America, 2013, p. 5.

[42] *ASTM International: Standard Test Methods for Elevated Temperature Tension Tests of Metallic Materials*, E21−09, 2009.

[43] (May, 2014). *Mikrotron High-Speed Kameras*. [En ligne]. Disponible: http://www.mikrotron.de/en/high-speed-camera-solutions/high-speed-recording-cameras/motionblitzr-cube.html

[44] "NI-Datasheet, Bus-Powered M Series Multifunction DAQ for USB," N. Instruments, Édit., éd. United States: National Instruments, 2012.

[45] *ASTM International: Standard Test Methods for Tension Testing of Metallic Materials*, E8/E8M-13a, 2009.

[46] "LM78XX Series Voltage Regulators," N. S. Corporation, Édit., éd: National Semiconductor Corporation, 2000, p. 7.

[47] *ASTM International: Standard Test Methods for Measuring and Compensating for Emissivity Using Infrared Imaging Radiometers*, E1933-99a, 2010.

[48] G. Greene et al., "Total hemispherical emissivity of oxidized Inconel 718 in the temperature range 300–1000° C," vol. 22, no. 3, p. 145-153, 2000.

[49] W. Owczaski et al., "Model for heat-affected zone cracking in Ni-Base superalloys," vol. 45, no. 4, p. 145-155, 1966.